

**ANALYSIS OF DAMPED LINEAR DYNAMIC SYSTEMS AND
APPLICATION OF COMPONENT MODE SYNTHESIS**

By

Alexander Muravyov

B.A.Sc., Chelyabinsk Polytechnic Institute, Russia, 1982

**A THESIS SUBMITTED IN PARTIAL FULFILLMENT OF
THE REQUIREMENTS FOR THE DEGREE OF
MASTER OF APPLIED SCIENCE**

in

**THE FACULTY OF GRADUATE STUDIES
DEPARTMENT OF MECHANICAL ENGINEERING**

We accept this thesis as conforming
to the required standard

THE UNIVERSITY OF BRITISH COLUMBIA

April 1994

© Alexander Muravyov, 1994

In presenting this thesis in partial fulfilment of the requirements for an advanced degree at the University of British Columbia, I agree that the Library shall make it freely available for reference and study. I further agree that permission for extensive copying of this thesis for scholarly purposes may be granted by the head of my department or by his or her representatives. It is understood that copying or publication of this thesis for financial gain shall not be allowed without my written permission.

(Signature)

Department of Mechanical Engineering

The University of British Columbia
Vancouver, Canada

Date April 25, 1994

Abstract

The analysis of nongyroscopic damped (viscous) linear dynamic systems is presented. Discrete systems having symmetric mass, stiffness and damping matrices are considered. Discretization of the systems is accomplished by application of the finite element procedure.

The general case of classically damped systems is considered, and the necessary and sufficient condition for classical damping is given. For a system of this type, it is possible to specify the damping matrix that will result in each mode having either a prescribed decay factor or a damped eigenfrequency. This may be accomplished with only a knowledge of the undamped eigenfrequencies. The equations required to accomplish this task are presented. Graphical results are presented that illustrate the effect of damping for mass-proportional, stiffness-proportional and for Rayleigh damping.

Nonclassically damped systems are considered and the formulation of a component mode synthesis (CMS) method for the solution of the free vibration problem is described.

The component mode synthesis method is a procedure in which the exact solution is approximated by one constructed from some basis vectors (e.g., mode shapes) of subsystems (components of the original system). This method allows significant reduction of the eigenvalue equation size due to the use of a limited number of basis vectors. The approximate solution found for the lower eigenvalues and eigenvectors is very close to the exact one due to the proper selection of the basis vectors and the procedure followed (e.g., Galerkin's method) that determines the best approximation. The use of CMS methods is especially advantageous in the case of large systems, subjected to numerous modifications.

In this work the formulation of the CMS method was developed for the general case of nonclassically damped systems. It was tested for different cases of nonclassically damped systems and the excellent agreement with the exact results derived from nonsubdivided systems was found. Also a new method to treat an unconstrained component for the purpose of stiffness matrix inversion is presented. The selection procedure of component modes is generalized from the undamped system case to the damped one.

Some examples of forced responses are considered, particularly, the case of sinusoidal excitation and the influence of the damping factor is analyzed.

The experimental part of this study consists of the designing and testing of a vibration rig designed to simulate the behaviour of a rigid engine resting on isolators that in turn are supported on flexible beams. Free and steady-state responses of the rig are experimentally determined.

Comparison of analytical results with experimental ones show good agreement for eigenquantities and steady-state forced response.

Table of Contents

Abstract	ii
Table of Contents	iv
List of Tables	vi
List of Figures	vii
List of Symbols	ix
Acknowledgement	xi
1 Introduction	1
1.1 Objectives	1
1.2 Background	1
1.2.1 Undamped systems	1
1.2.2 Classically damped systems	3
1.2.3 Nonclassically damped systems	4
2 Analysis of damped systems	7
2.1 Classically damped systems	7
2.2 Nonclassically damped systems	15
2.3 Free response function computation	17
2.4 Steady-state response function computation	18

3	Formulation of component mode synthesis method	25
3.1	Undamped systems	25
3.1.1	Case of an unconstrained component. Method of weak springs . .	31
3.2	Nonclassically damped systems	34
3.2.1	Component mode selection procedure	40
3.3	Case of an arbitrary number of components	42
4	Numerical results	45
4.1	Comparison of CMSFR method with "VAST" program for undamped systems	45
4.2	Comparison of CMSFR method with "DREIGN" program for undamped and nonclassically damped systems	50
5	Experimental results	56
6	Summary	64
	Bibliography	66
A	User's Manual for the CMSFR method	69
B	Parameters of the vibration rig	73

List of Tables

2.1	Steady-state responses, examples 1,2	23
2.2	Steady-state responses, examples 3,4	23
2.3	Steady-state responses, examples 5,6	23
4.1	Four component beam element system: "a"	47
4.2	Three component beam-bar element system with one rigid-body mode: "b"	47
4.3	Three component beam-bar-membrane element system: "c"	48
4.4	Four component beam-brick element system: "d"	48
4.5	Two component beam element system	51
4.6	System with dashpots and lumped masses	52
4.7	Comparison of eigenvalues for the undamped rig model	53
4.8	Comparison of the 1st eigenvectors for the undamped rig model	54
4.9	Comparison of eigenvalues for the damped rig model	55
4.10	Comparison of the 1st eigenvectors for the damped rig model	55
5.1	Stiffness and damping properties of the spring isolators (undamped rig)	58
5.2	Stiffness and damping properties of the spring isolators (damped rig)	58
5.3	Experimental frequencies for two rig tests	59
5.4	Amplitudes, Phase angles for undamped rig	60
5.5	Amplitudes, Phase angles for undamped rig ... continued	62
5.6	Amplitudes, Phase angles for damped rig	62
5.7	Amplitudes, Phase angles for damped rig ... continued	63

List of Figures

2.1	Effect of mass-proportional damping	13
2.2	Effect of stiffness-proportional damping	14
2.3	Effect of Rayleigh damping	15
2.4	Two degree of freedom system	16
2.5	Eigenvalues of the system in Fig 2.4	17
2.6	Model of the rig with selected nodes	22
2.7	Effect of damping on transmissibility	24
3.1	Two component system	26
3.2	Linear bar element	32
3.3	Mode selection procedure	41
4.1	Test examples	46
4.2	First mode shape of the system in Fig.4.1,a	49
4.3	Second mode shape of the system in Fig.4.1,a	49
4.4	Two component beam element system	50
4.5	System with dashpots and lumped masses	52
4.6	Finite element model of the rig	52
4.7	Four component presentation of the system	53
4.8	Selected nodes for the eigenvector presentation	54
5.1	Photo of the experimental rig	57
5.2	Reference points on the test rig	58

5.3 Spring isolator characteristic determination 59

5.4 8 - 24 Hz excitation sweep 61

B.1 Vibration rig, side view 73

B.2 Vibration rig, front view 74

B.3 Vibration rig, top view of the box 75

List of Symbols

M	mass matrix of system
K	stiffness matrix of system
C	damping matrix of system
λ	system eigenvalue
ϕ	system eigenvector
Φ	matrix of mode shapes
X	displacement vector of system
p	vector of modal coordinates
F	external force vector, acting on system
F_c	vector of forces acting on components
m_1	mass matrix of 1st component
k_1	stiffness matrix of 1st component
c_1	damping matrix of 1st component
m_2	mass matrix of 2nd component
k_2	stiffness matrix of 2nd component
c_2	damping matrix of 2nd component
ϕ_1	subvector of system eigenvector for 1st component
ϕ_2	subvector of system eigenvector for 2nd component
f_1	force vector acting on 1st component
f_2	force vector acting on 2nd component
Φ_1^l	matrix of lower (retained) free-free modes of 1st component
Φ_2^l	matrix of lower (retained) free-free modes of 2nd component

Φ_1^α	matrix of residual-attachment modes of 1st component
Φ_2^α	matrix of residual-attachment modes of 2nd component
p_1^l	vector of free-free mode coordinates for 1st component
p_2^l	vector of free-free mode coordinates for 2nd component
p_1^α	vector of residual-attachment mode coordinates for 1st component
p_2^α	vector of residual-attachment mode coordinates for 2nd component

All the remaining notations are described as they occur in the text.

Acknowledgement

The author would like to offer sincere thanks to Professor Stanley G. Hutton for his insight and advices in the preparation of this thesis. The author would like also to acknowledge the financial support provided by Defense Research Establishment Atlantic.

Chapter 1

Introduction

1.1 Objectives

The objectives of the present research can be formulated as:

- 1) investigating the conditions which lead to classically damped vibratory systems,
- 2) analysis of nonclassically damped systems,
- 3) development of a component mode synthesis method for analysing the free and steady-state responses of nonclassically damped systems,
- 4) construction of an experimental model to investigate the effect of damping upon the system response; data acquisition, analysis of experimental results and comparison with the analytical ones,
- 5) investigating the effect on transmissibility of the damping characteristics of spring isolators of the type used to isolate engine vibrations.

1.2 Background

1.2.1 Undamped systems

The literature on applications of component mode synthesis techniques to discrete undamped systems contains description of many different methods such as fixed-interface methods [1], [2], free-interface methods [3], [4], [5], [6], [7] and others [8], [9], [10],[11].

Before discussing existing CMS techniques it is expedient to give a little introduction concerned with the general idea of component mode synthesis.

Consider the system of equations of free motion of a discrete undamped system

$$M\ddot{X} + KX = 0$$

which leads to the eigenvalue equation

$$(-\omega^2 M + K)\phi = 0$$

where M = mass matrix, K = stiffness matrix of the system, ω = system eigenfrequency, ϕ = system eigenvector.

In CMS, the system is subdivided into a set of subsystems (components). Thus the system eigenvector (or displacement vector) defined on the entire domain occupied by the system can be partitioned into parts which are defined on the subdomains. Within a subdomain occupied by k th component the corresponding part of the system eigenvector (denote it by ϕ_k) is approximated by a linear combination of some basis vectors Φ^l (in general different for each component):

$$\phi_k = \Phi^l p_k^l$$

where p_k^l is a subset of the system generalized coordinates associated with k th component.

CMS methods differ to some extent in the selection of these vectors. The basis vectors used can be classified into the following groups: 1) free-free vibration modes, 2) fixed-interface vibration modes (by interface is meant a common boundary between adjacent components), 3) attachment modes, 4) constraint modes, 5) residual-attachment modes, 6) rigid-body modes. Free-free and fixed-interface modes are obtained by the solution of corresponding eigenproblems for free, or fixed (clamped) interface components. Constraint and attachment modes are respectively vectors of static displacements caused by a unit displacement, or unit load applied at the interface. The definition of residual-attachment modes will be given in chapter 3.

The combination of free-free modes (including rigid-body modes) with residual-attachment ones is usually viewed as a free-interface method. The fixed-interface method uses fixed-interface vibration modes with constraint (or attachment) modes, plus rigid-body modes. A review and comparison of fixed- and free-interface methods has been conducted by a number of authors [2], [9], [12], [13].

In [14], [15], the use of a set of admissible functions different to vibration modes is proposed, e.g., low order polynomial functions. This gives an opportunity to avoid eigensolutions at the component level. For discrete systems these polynomial functions are replaced by their values at the nodes of the system, i.e. by vectors. However the choice of these functions seems to be problematic. For 3-D systems with complex geometry, boundary conditions, nonuniform mass and stiffness distribution it is not clear how many such basis vectors would be required for an accurate approximation.

1.2.2 Classically damped systems

Description of this type of system can be found in many references, e.g., [16], [11], [17], [18], [19], [20]. Usually consideration was limited to systems having Rayleigh damping $C = \alpha M + \beta K$, where α and β are constants. The necessary and sufficient conditions when a system has classical normal modes (the eigenvectors are the same for damped and undamped systems, i.e. they are real vectors) was formulated in [21],[22] as $M^{-1}C$ commutes with $M^{-1}K$, where C = damping matrix of the system.

The analysis of this type of system is considered in chapter 2. For a system with distinct undamped natural frequencies the necessary and sufficient condition of proportionality for C will be given in section 2.1 in terms of matrices M, K .

Note that application of CMS methods to this kind of system can be accomplished by: i) application to the associated undamped system ($C = 0$), ii) construction of undamped system eigenvector of interest ϕ , iii) computation of system eigenvalue λ (complex) of

interest from the equation

$$\lambda^2 \phi^T M \phi + \lambda \phi^T C \phi + \phi^T K \phi = 0$$

When structural damping is considered (usually related with sinusoidal excitation of a given frequency) the equivalent viscous damping matrix can be determined. In this case it is taken as proportional to the stiffness matrix and inversely proportional to the excitation frequency. Description of this type of damping can be found in [23] for example.

1.2.3 Nonclassically damped systems

There have been some efforts to develop CMS methods for nonclassically damped systems in the past, though there is very little literature on this topic.

The system of equations of free motion of the system is expressed as following:

$$M\ddot{X} + C\dot{X} + KX = 0 \tag{1.1}$$

where the damping matrix cannot be diagonalized simultaneously with M and K .

One approach assumes that the system is lightly, or proportionally damped [1], [2], [11] and the system eigenvector is constructed from undamped vibration modes (real vectors) of components. This representation does not take into account the damping properties of the components and cannot be accurate, especially in the case of significant damping.

To solve the eigenvalue problem for a nonclassically damped system it is expedient to rewrite the equation of free motion (1.1) in the reduced, or so-called state-space form:

$$A\dot{Y} + BY = 0 \tag{1.2}$$

$$\text{where } A = \begin{bmatrix} C & M \\ M & 0 \end{bmatrix}, B = \begin{bmatrix} K & 0 \\ 0 & -M \end{bmatrix}, Y = \begin{bmatrix} X \\ \dot{X} \end{bmatrix}.$$

Equation (1.2) leads to the eigenvalue equation

$$(\lambda A + B)\phi = 0$$

which yields complex eigenvalues λ and complex state-space eigenvectors ϕ .

Hale [15] proposed to use vibration modes of undamped components and to improve accuracy by iteratively generating component state-space vectors. Hasselman and Kaplan [24] used complex vibration modes, but it was not shown how they were determined and the residual-attachment modes were not taken into account. In [25] a modified fixed-interface method is shown, where fixed-interface vibration modes of undamped components are replaced by corresponding complex modes.

Howsman and Craig [26] showed a state-space free-interface formulation that uses a set of free-interface vibration modes, but instead of residual-attachment modes a set of attachment modes was used.

Another application of a state-space free-interface CMS technique for nonclassically damped systems was shown in [27] for the case of a two component system, where along with free-interface vibration modes a set of residual-attachment modes was used. This formulation has similarity (in terms of coupling procedure) with the formulation developed in this thesis, however in [27] the selection of free-free vibration modes was not generalized from the undamped system case to the damped one and the authors used different approach for determination of residual-attachment modes in the case of unconstrained components.

In this thesis a formulation of state-space free-interface method (CMSFR) has been developed for systems with nonclassical damping for the case when mass, stiffness and damping matrices of components are symmetric. A system eigenvector is constructed

from state-space free-free vibration modes of damped components and state-space residual-attachment modes. A complex eigensolver is used to determine the free-free vibration modes of each component. The formulation is demonstrated for an arbitrary number of components, which can be constrained or unconstrained. Also a new method is presented to treat an unconstrained component, which is more economical in the computational sense than the method shown in [27]. A selection procedure for the retained free-interface vibration modes is developed for this nonclassically damped system case.

Chapter 2

Analysis of damped systems

2.1 Classically damped systems

In this chapter, unsubdivided systems are considered. The general case of classical damping is analysed. An important property of this kind of damped system is that it has classical mode shapes (eigenvectors), i.e, the same as the associated undamped system.

The system of equations of free vibration of a discrete nongyroscopic damped system can be expressed in the form

$$M\ddot{X} + C\dot{X} + KX = 0 \quad (2.1)$$

where M, C, K represent mass, damping and stiffness matrices of order N . Under certain conditions this system of, in general, coupled differential equations can be transformed to a system of uncoupled equations by a congruence transformation. It is known that the mode shape matrix of the undamped system can make this transformation with respect to the M and K matrices. In this study the necessary and sufficient condition of diagonalization of C by this matrix of undamped mode shapes is considered. For a general system it has been formulated, e.g., in [21], [22] as $M^{-1}C$ commutes with $M^{-1}K$.

It should be noted that the necessary and sufficient condition for diagonalization of matrix C in terms of undamped system modes Φ

$$\Phi^T C \Phi = [a_i],$$

or

$$C = (\Phi^T)^{-1} [a_i] \Phi^{-1}$$

($[a_i]$ is a diagonal matrix) implies that N real coefficients a_i is enough to describe all the variety of possible damping matrices for the given system defined by M, K .

Limiting consideration to systems that have distinct (no repeated) undamped natural frequencies the necessary and sufficient condition of proportionality imposed on matrix C will be formulated in terms of matrices M, K (M is positive definite and K is positive semidefinite) in the theorem below.

Theorem.

For the given matrices M, K of order N in (2.1) the matrix C will be diagonalized simultaneously with M, K if, and only if, it is represented as

$$C = M \sum_{l=1}^N g_l (M^{-1}K)^{l-1} \quad (2.2)$$

where $g_l, l = 1, 2, \dots, N$ are arbitrary coefficients.

Proof.

Necessity.

There is such a matrix Φ consisting of undamped mode shapes that

$$\Phi^T M \Phi = I$$

$$\Phi^T K \Phi = [b_i]$$

$$\Phi^T C \Phi = [a_i]$$

where $[b_i] = b, [a_i] = a$ are diagonal matrices and the matrix Φ is mass normalized (first equation), so the elements of b will be the natural frequencies squared. Rewrite the above expressions as

$$C = (\Phi^T)^{-1} a \Phi^{-1} \quad (2.3)$$

$$K = (\Phi^T)^{-1} b \Phi^{-1} \quad (2.4)$$

and

$$M = (\Phi\Phi^T)^{-1} \quad (2.5)$$

or

$$M^{-1} = \Phi\Phi^T \quad (2.6)$$

It is obvious that there is one to one mapping, namely, $a \rightarrow \leftarrow C$, $b \rightarrow \leftarrow K$. Express matrix a as

$$a = g_1 I + g_2 b + \dots + g_N b^{N-1} \quad (2.7)$$

Equation (2.7) can be rewritten as a system of linear equations for coefficients g_k , $k = 1, 2, \dots, N$

$$\begin{bmatrix} 1 & b_1 & b_1^2 & \dots & b_1^{N-1} \\ 1 & b_2 & b_2^2 & \dots & b_2^{N-1} \\ \dots & \dots & \dots & \dots & \dots \\ 1 & b_N & b_N^2 & \dots & b_N^{N-1} \end{bmatrix} \begin{bmatrix} g_1 \\ g_2 \\ \cdot \\ \cdot \\ g_N \end{bmatrix} = \begin{bmatrix} a_1 \\ a_2 \\ \cdot \\ \cdot \\ a_N \end{bmatrix} \quad (2.8)$$

The determinant of this system (the Vandermonde determinant) is non-zero because there are no repeated values b_i (natural frequencies squared), so the solution is guaranteed and this representation (2.7) holds. Rewrite (2.7) using (2.3),(2.4)

$$\Phi^T C \Phi = \sum_{k=1}^N g_k (\Phi^T K \Phi)^{k-1}$$

Therefore any matrix C can be represented as

$$C = (\Phi^T)^{-1} [g_1 I + g_2 \Phi^T K \Phi + g_3 \Phi^T K \Phi \Phi^T K \Phi + \dots + g_N \Phi^T K \Phi \dots \Phi^T K \Phi] \Phi^{-1}$$

and using (2.6) one can obtain

$$C = M \sum_{l=1}^N g_l (M^{-1} K)^{l-1}$$

as required.

Sufficiency.

The damping matrix is given as in (2.2). Using (2.5),(2.6),(2.4) one can obtain

$$\begin{aligned} C &= (\Phi\Phi^T)^{-1} \sum_{l=1}^N g_l (\Phi\Phi^T(\Phi^T)^{-1}b\Phi^{-1})^{l-1} = \\ &= (\Phi^T)^{-1}(g_1 + g_2b + \dots + g_Nb^{N-1})\Phi^{-1} \end{aligned}$$

Therefore

$$\Phi^T C \Phi = \sum_{l=1}^N g_l b^{l-1}$$

represents a diagonal matrix as a sum of diagonal matrices, which was required to prove.

It may seen from (2.2) that if the first two terms are taken then

$$C = g_1 M + g_2 K \quad l = 1, 2$$

which is Rayleigh damping. If more terms taken, e.g. three, then

$$C = g_1 M + g_2 K + g_3 K M^{-1} K \quad l = 1, 2, 3$$

and so on.

Remark 1.

Note that for systems with repeated undamped natural frequencies expression (2.2) will represent a sufficient condition, but not the necessary one. This means that there might be matrices C , which are not represented as in (2.2), but are diagonalizable.

Remark 2.

For a system with repeated undamped eigenvalues the representation (2.2) will hold as the necessary condition if the vector of damping coefficients $[a_k]$ lies in the space of eigenvectors of the system matrix (2.8). Then, for example, if there are m repeated eigenvalues it means that eigenvectors of the Vandermonde matrix will represent the

vector subspace dimensioned by $N - m + 1$. The form of these eigenvectors is not considered here and an explicit expression of vector $[a_k]$ as a linear combination of these eigenvectors is not shown. It is left to note that in this case there will be an infinite number of solutions (vectors $[g_k]$) which yield the given damping coefficient vector $[a_k]$.

Consider now the general case of classical damping for a system with distinct undamped natural frequencies. Substituting (2.2) in (2.1) and using the transformation to modal coordinates $X = \Phi p$ with premultiplication by Φ^T gives:

$$\Phi^T M \Phi \ddot{p} + \Phi^T [M \sum_{k=1}^N g_k (M^{-1} K)^{k-1}] \Phi \dot{p} + \Phi^T K \Phi p = 0 \quad (2.9)$$

where Φ is the matrix of classical mode shapes. Assuming that Φ is mass normalized then

$$\Phi^T M \Phi = I, \quad \Phi^T K \Phi = \Lambda$$

where Λ is a diagonal matrix, whose elements are the undamped natural frequencies squared $\eta_i = \omega_i^2$. The matrix equation (2.9) can then be written as a system of uncoupled equations:

$$\ddot{p}_i + \left(\sum_{k=1}^N g_k \eta_i^{k-1} \right) \dot{p}_i + \eta_i p_i = 0 \quad i = 1, 2, \dots, N \quad (2.10)$$

Equations (2.10) yield the eigenvalues of the damped system, namely:

$$\lambda_{i+} = \frac{1}{2} \left(- \sum_{k=1}^N g_k \eta_i^{k-1} + \sqrt{D} \right), \quad \lambda_{i-} = \frac{1}{2} \left(- \sum_{k=1}^N g_k \eta_i^{k-1} - \sqrt{D} \right)$$

where $D = \left(\sum_{k=1}^N g_k \eta_i^{k-1} \right)^2 - 4\eta_i$. If $D < 0$ the roots are complex conjugate, otherwise they are real.

Considering the case of complex conjugate roots:

$$Re(\lambda_i) = -\frac{1}{2} \sum_{k=1}^N g_k \eta_i^{k-1} \quad (2.11)$$

and

$$Im(\lambda_i) = \frac{1}{2} \sqrt{-D} = \sqrt{\eta_i - \frac{1}{4} \left(\sum_{k=1}^N g_k \eta_i^{k-1} \right)^2} \quad (2.12)$$

From which it may be seen that

$$(Re(\lambda_i))^2 + (Im(\lambda_i))^2 = \eta_i = \omega_i^2 \quad (2.13)$$

Therefore the absolute values of complex eigenvalues are independent of arbitrary proportional damping. It may also be noted from (2.12) that for classical damping the damped natural frequencies are always less than the undamped frequencies.

If it is required to modify the natural frequencies of a given system by modification of the damping matrix, equations (2.11),(2.13) can be used to determine the coefficients g_k in (2.2) that yield the required eigenvalues. For example, upon the prescription of the imaginary parts of the first (lowest) L eigenvalues ($L = 1, \text{ or } 2, \dots, N$) equations (2.13) can be used to determine the corresponding real parts. Then the use of (2.11) yields the following system of algebraic equations for the kept (non-zero) coefficients g_k :

$$-\frac{1}{2} \begin{bmatrix} 1 & \eta_1 & \eta_1^2 & \dots & \eta_1^{L-1} \\ 1 & \eta_2 & \eta_2^2 & \dots & \eta_2^{L-1} \\ \dots & \dots & \dots & \dots & \dots \\ 1 & \eta_L & \eta_L^2 & \dots & \eta_L^{L-1} \end{bmatrix} \begin{bmatrix} g_1 \\ g_2 \\ \dots \\ g_L \end{bmatrix} = \begin{bmatrix} Re(\lambda_1) \\ Re(\lambda_2) \\ \dots \\ Re(\lambda_L) \end{bmatrix}$$

The determinant of this system is the Vandermonde determinant, which is not zero if there are no repeated η_i . Therefore for a system with distinct undamped natural frequencies there will be a unique solution for g_k , $k = 1, 2, \dots, L$. Note that only a knowledge of undamped natural frequencies is necessary to construct the required C .

Three particular cases of proportional damping are now considered.

i) Mass-proportional damping: the damping matrix is represented as $C = \alpha M$, which corresponds to the case when all $g_i = 0$, except $g_1 = \alpha$. The effect of mass-proportional damping upon the damped frequency ($Im(\lambda_i)$) and decay factor ($Re(\lambda_i)$) is illustrated graphically in Figure 2.1. The undamped natural frequencies ω_{min} , ω_i and ω_{max} represent respectively the minimum, some intermediate and the maximum value for the system with

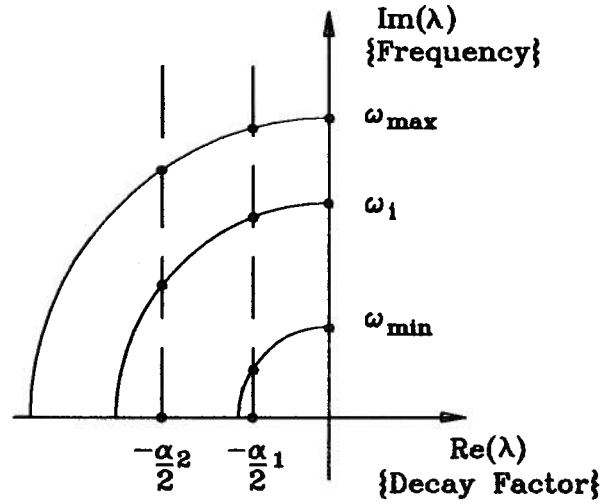


Figure 2.1: Effect of mass-proportional damping

no damping. The equation (2.13) is shown by solid circles, while the dashed lines represent equation (2.11). Intersection of the solid circles with the dashed lines corresponds to the location of eigenvalues. If no intersection occurs that mode is overdamped for that value of damping. Thus if $\alpha < 2\omega_{min}$ all modes are oscillatory and if $\alpha > 2\omega_{max}$ all modes are overdamped. It may be observed that mass-proportional damping has a larger influence on the lower mode frequencies than those of the higher modes.

ii) Stiffness-proportional damping: the damping matrix is represented in this case as $C = \beta K$, corresponding to the case when all $g_i = 0$, except $g_2 = \beta$. To illustrate the effect of stiffness-proportional damping introduce the following notations: $x = Re(\lambda_i)$, $y = Im(\lambda_i)$. Equations (2.11),(2.12) lead to

$$y^2 + (x + 1/\beta)^2 = 1/\beta^2$$

which represents the equation of circles shown as dashed circles in Figure 2.2. Equations (2.13) are shown by solid circles and upon the given β the eigenvalue location is determined by the intersection of the corresponding dashed circle with the solid ones. In this case it may be seen that the stiffness-proportional damping has a larger influence on the

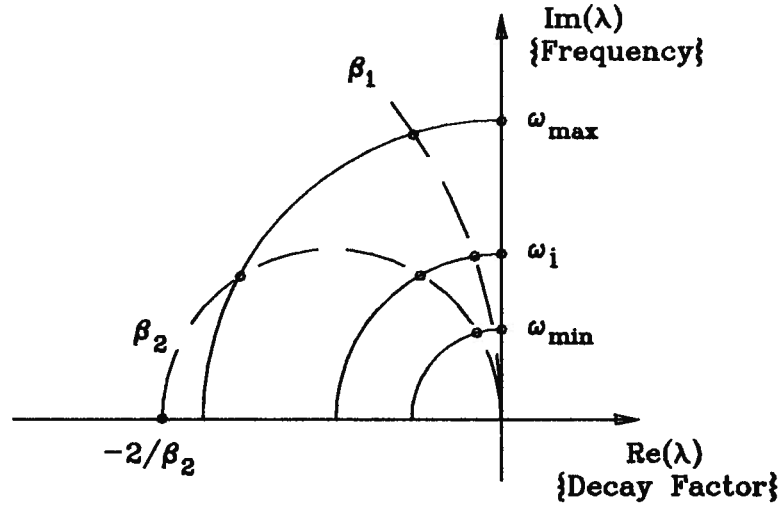


Figure 2.2: Effect of stiffness-proportional damping

higher mode frequencies. From the figure it may be noted that if $\beta > \frac{2}{\omega_{min}}$ all modes are overdamped and if $\beta < \frac{2}{\omega_{max}}$ all modes are oscillatory.

iii) Rayleigh damping $g_1 = \alpha$, $g_2 = \beta$, i.e., $C = \alpha M + \beta K$.

Using the same notations equations (2.11),(2.12) lead to

$$y^2 + (x + 1/\beta)^2 = (1 - \alpha\beta)/\beta^2$$

The graphs of these circles are shown as dashed lines in Figure 2.3. Upon the given α, β the eigenvalue location is determined once again by the intersection of the corresponding dashed circle with the solid ones. Intersection of dashed circle with x axis gives two values: $x_R = \frac{-1 + \sqrt{1 - \alpha\beta}}{\beta}$, $x_L = \frac{-1 - \sqrt{1 - \alpha\beta}}{\beta}$. The condition that all the modes are oscillatory is the simultaneous satisfaction of the following inequalities: $\frac{1 - \sqrt{1 - \alpha\beta}}{\beta} < \omega_{min}$ and $\frac{1 + \sqrt{1 - \alpha\beta}}{\beta} > \omega_{max}$. If $\frac{1 - \sqrt{1 - \alpha\beta}}{\beta} > \omega_{max}$, or $\frac{1 + \sqrt{1 - \alpha\beta}}{\beta} < \omega_{min}$, or $\alpha\beta > 1$ all modes are overdamped. Note that at $\alpha\beta = 1$ the radius of the dashed circle becomes zero.

It may seen from the figure that it is possible to choose Rayleigh damping coefficients such that the lowest and higher modes are overdamped, but the intermediate modes are oscillatory.

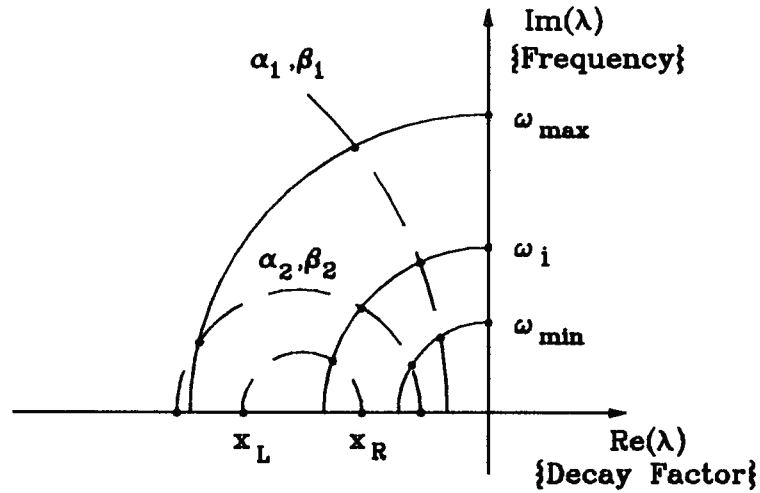


Figure 2.3: Effect of Rayleigh damping

2.2 Nonclassically damped systems

In the case of nonclassically damped systems the general damping matrix cannot be expressed in the form defined by equation (2.2). The damping matrix of this type of system cannot be diagonalized simultaneously with M and K . To solve the eigenvalue problem it is expedient to rewrite equation (2.1) in the reduced or so-called state-space form:

$$A\dot{Y} + BY = 0 \quad (2.14)$$

where

$$A = \begin{bmatrix} C & M \\ M & 0 \end{bmatrix}, \quad B = \begin{bmatrix} K & 0 \\ 0 & -M \end{bmatrix}, \quad Y = \begin{bmatrix} X \\ \dot{X} \end{bmatrix} \quad (2.15)$$

The equation of free motion in a system mode $Y(t) = e^{\lambda t}\phi$ with eigenvalue λ and state-space eigenvector ϕ will have the following form:

$$(\lambda A + B)\phi = 0 \quad (2.16)$$

where A , B are real symmetric $2N \times 2N$ matrices, which are not positive definite. Note that the eigenvectors will be orthogonal with respect to A , B . The eigenvectors ϕ_i can

be normalized by setting

$$\phi_i^T A \phi_i = 1 \quad i = 1, 2, \dots, 2N$$

or if Φ is defined as a matrix of A-normalized eigenvectors, then the following will hold:

$$\Phi^T A \Phi = I \quad \Phi^T B \Phi = -\Lambda$$

where Λ is the diagonal matrix of eigenvalues.

There are different numerical methods for the solution of such a kind of eigenproblems. The solution of this problem can be found, e.g., using the QR method [28], [29]. In general there will be $2m$ real eigenvalues and $N - m$ pairs of complex conjugate ones.

The influence of damping on the response is complicated as the eigenvectors themselves depend upon C . To illustrate the effect of nonclassical damping the behaviour of the simple system shown in Figure 2.4 is analyzed, where $m_1 = m_2 = k_1 = k_2 = 1$. The location of eigenvalues for different values of c is shown in Figure 2.5.

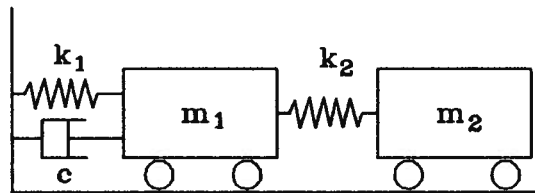


Figure 2.4: Two degree of freedom system

As may be noted the behaviour is quite different to that of a classically damped system. As the damping constant c is first increased the imaginary part (frequency) of the lowest eigenvalue increases (a phenomenon not observed in classically damped systems) and that of the higher mode decreases. The real parts both increase with c up to a certain point after which the real part of the second mode begin to decrease. At a damping value of 2 both roots coincide and at this point there is a discontinuity in the

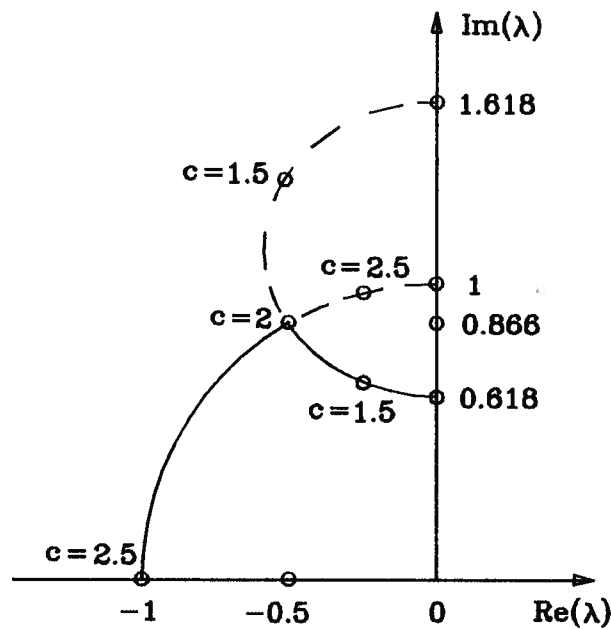


Figure 2.5: Eigenvalues of the system in Fig 2.4

monotonic behaviour of the eigenvalues. The imaginary part (frequency) of the second eigenvalue then starts to increase monotonically to a frequency of 1 rad/s . This situation corresponds to the physical condition when c is so high that the first mass does not move and the system is responding essentially as a single degree of freedom system. The real part of the first eigenvalue monotonically increases and at $c = 2.5$ this mode becomes critically damped.

2.3 Free response function computation

Consider a homogeneous equation of motion of a nonclassically damped system with N degrees of freedom:

$$M\ddot{X} + C\dot{X} + KX = 0$$

To find a homogeneous solution the eigenproblem should be solved first. The solution of eigenproblem is usually conducted by application of the state-space representation (2.14)-(2.16). Note that eigenvalues and eigenvectors of this problem are in general complex. The homogeneous solution will be presented in a complex form

$$Y = \sum_{j=1}^{2N} A_j e^{\lambda_j t} \phi_j \quad (2.17)$$

where λ_j , ϕ_j are the eigenvalues and eigenvectors and A_j are complex coefficients.

The real form solution can be extracted from (2.17). Assume in general there is $2m$ real eigenvalues and $N - m$ pairs of complex conjugate ones, then the real homogeneous solution X_{hom} can be presented as

$$X_{hom}(t) = \sum_{k=1}^{2m} c_k e^{\lambda_k^r t} \text{Re}[\phi_k^r] + \sum_{j=1}^{N-m} c_{2m+j} \text{Re}[e^{\lambda_j^c t} \phi_j^c] + \sum_{j=1}^{N-m} c_{N+m+j} \text{Im}[e^{\lambda_j^c t} \phi_j^c]$$

where λ_k^r are $2m$ real eigenvalues and λ_j^c are $N - m$ representatives of complex conjugate eigenvalues, ϕ_k^r , ϕ_j^c are the corresponding complex state-space eigenvectors. The real coefficients c_k , $k = 1, 2, \dots, 2N$ will be determined from the initial condition

$$X_{hom}(0) = X(0) - X_{par}(0)$$

which represents the system of $2N$ real linear equations, where X is the total solution and X_{par} a particular term (in the case of external force presence) of the solution.

2.4 Steady-state response function computation

The forced response due to a sinusoidal excitation is considered in this section. In the experimental part of this work this type of excitation will be considered. The equation of motion of a nonclassically damped system:

$$M\ddot{X} + C\dot{X} + KX = F(t) \quad (2.18)$$

where the external force vector

$$F(t) = F_0 \sin \omega t \quad (2.19)$$

Although steady-state response X can be found from (2.18) directly, the state-space representation will be used to show the relation between complex and real forms of the solution:

$$A\dot{Y} + BY = F_{st} \quad (2.20)$$

$$\text{where } A = \begin{bmatrix} C & M \\ M & 0 \end{bmatrix}, B = \begin{bmatrix} K & 0 \\ 0 & -M \end{bmatrix}, Y = \begin{bmatrix} Y_d \\ \dot{Y}_d \end{bmatrix}, F_{st} = \begin{bmatrix} F_d(t) \\ 0 \end{bmatrix}.$$

The seeking complex solution is

$$Y_d = (Y_1 + iY_2)e^{i\omega t} \quad (2.21)$$

as the response to a given complex force

$$F_d = (f_1 + if_2)e^{i\omega t} = f_1 \cos \omega t - f_2 \sin \omega t + i(f_1 \sin \omega t + f_2 \cos \omega t) \quad (2.22)$$

The steady-state response in real form may be expressed as

$$X = \text{Re}[Y_d] \quad (2.23)$$

or

$$X = \text{Im}[Y_d]$$

Proceeding with (2.23) the given force will be

$$F(t) = \text{Re}[F_d] = f_1 \cos \omega t - f_2 \sin \omega t$$

In the case (2.19)

$$f_1 = 0 \quad (2.24)$$

$$f_2 = -F_0 \quad (2.25)$$

Substituting (2.21),(2.22) in (2.20) and cancelling $e^{i\omega t}$ one can obtain

$$\begin{bmatrix} C & M \end{bmatrix} \begin{bmatrix} (Y_1 + iY_2)i\omega \\ -(Y_1 + iY_2)\omega^2 \end{bmatrix} + \begin{bmatrix} K & 0 \end{bmatrix} \begin{bmatrix} Y_1 + iY_2 \\ (Y_1 + iY_2)i\omega \end{bmatrix} = (f_1 + if_2) \quad (2.26)$$

Rewriting equation (2.26) as

$$Y_1(-M\omega^2 + K) - Y_2C\omega + i(Y_1C\omega + Y_2(-M\omega^2 + K)) = f_1 + if_2$$

one can obtain the system of linear equations for Y_1, Y_2 (taking into account (2.24),(2.25))

$$\begin{bmatrix} C\omega & -M\omega^2 + K \\ -M\omega^2 + K & -C\omega \end{bmatrix} \begin{bmatrix} Y_1 \\ Y_2 \end{bmatrix} = \begin{bmatrix} -F_0 \\ 0 \end{bmatrix} \quad (2.27)$$

The solution of (2.27) yields the steady-state response

$$X = \text{Re}[(Y_1 + iY_2)e^{i\omega t}] = Y_1 \cos \omega t - Y_2 \sin \omega t$$

which can be presented in the following form

$$X = D \sin(\omega t + \psi)$$

where

$$D = \begin{bmatrix} d_1 & d_2 & \dots & d_N \end{bmatrix}^T$$

is the amplitude vector of the forced response and

$$\psi = \begin{bmatrix} \psi_1 & \psi_2 & \dots & \psi_N \end{bmatrix}^T$$

is the phase angle vector. In more detail

$$d_i = \sqrt{Y_{1i}^2 + Y_{2i}^2}$$

and

$$\tan \psi_i = -\frac{Y_{1i}}{Y_{2i}}$$

where Y_{1i} , Y_{2i} are i th components of vectors Y_1 , Y_2 respectively.

Remark 1.

Note that system matrix of (2.27) (denote it by S) can be inverted in the following ways: i) if damping matrix $C = 0$, then

$$S^{-1} = \begin{bmatrix} 0 & (-M\omega^2 + K)^{-1} \\ (-M\omega^2 + K)^{-1} & 0 \end{bmatrix}$$

ii) if C is not a zero matrix and assumed invertible, then

$$S^{-1} = \begin{bmatrix} a_{11} & a_{12} \\ a_{12} & -a_{11} \end{bmatrix},$$

where $a_{11} = G^{-1}(DG^{-1} + GD^{-1})^{-1}$, $a_{12} = a_{11}GD^{-1}$, $D = C\omega$, $G = -M\omega^2 + K$. This leads to economy of computer time because the inversion of a matrix $2N$ by $2N$ is replaced by inversion of a matrix N by N in case i) and by three inversions of a matrix N by N in case ii).

Below some numerical results are presented, which show the influence of damping on the steady-state vibration response. As an illustration a finite element model of the vibration rig (Fig.2.6) was considered. Parameters of the rig are presented in Appendix B. A vertical concentrated load $F = F_0 \sin \omega t$ was applied at the centre of the box, where $F_0 = 30 \text{ N}$ and $\omega = 32 \text{ Hz}$ were the same for all examples. Of interest is the influence of damping properties in the spring elements a, b, c, d . The following values of a damping constant were assigned: 1) $c = 0$ (undamped system), 2) $c = 0.002k_s$, 3) $c = 0.005k_s$, 4) $c = 0.01k_s$, 5) $c = 0.02k_s$, 6) $c = 0.05k_s$, where $k_s = 12 \text{ N/mm}$ was the vertical axial stiffness of the elements a, b, c, d and kept constant. The influence of c upon the response of the system was analyzed. For the chosen nodes (Fig.2.6) the amplitudes and phase angles were computed and the results for the vertical component of motion are shown in Tables 2.1-2.3.

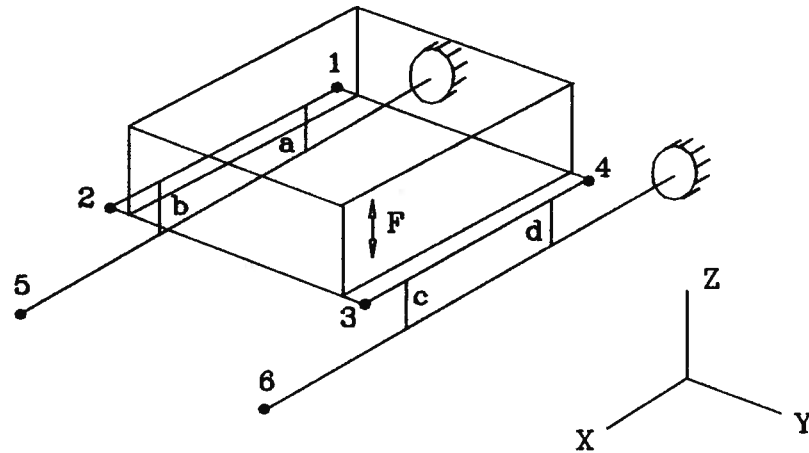


Figure 2.6: Model of the rig with selected nodes

It may be noted from Tables 2.1-2.3 that amplitudes of motion of points 5,6 are decreasing with increase of c and phase angles change.

The ratio A_{sup}/A_{box} was calculated, where A_{box} is the amplitude of vertical motion at the centre of the box and A_{sup} is the amplitude of vertical motion of the supported beams (the average amplitude of the points 5,6 was taken). This ratio characterizes the transmissibility of motion from the box (points 1-4) to the supported beams. The change of this transmissibility depending of c/k_s is presented in Fig. 2.7. It may be noted that increase of damping up to the $c = 0.01k_s$ leads to decrease of amplitudes of vibration of the supported beams, in other words provides decrease of transmissibility of motion from the box to the supported beams. After $c = 0.01k_s$ the influence of c upon transmissibility is insignificant, though the phase angles continue to change.

Node	<i>Example 1, $c = 0$</i>		<i>Example 2, $c = 0.002k_s$</i>	
	Amplitude, <i>mm</i>	Phase angle, $^\circ$	Amplitude, <i>mm</i>	Phase angle, $^\circ$
1	0.0280	180.	0.0261	183.
2	0.0306	180.	0.0242	188.
3	0.0324	180.	0.0261	188.
4	0.0264	180.	0.0241	184.
5	0.224	0.	0.116	82.7
6	0.228	0.	0.118	82.6

Table 2.1: Steady-state responses, examples 1,2

Node	<i>Example 3, $c = 0.005k_s$</i>		<i>Example 4, $c = 0.01k_s$</i>	
	Amplitude, <i>mm</i>	Phase angle, $^\circ$	Amplitude, <i>mm</i>	Phase angle, $^\circ$
1	0.0256	183.	0.0255	183.
2	0.0224	184.	0.0221	181.
3	0.0243	184.	0.0240	181.
4	0.0235	183.	0.0234	184.
5	0.0674	122.	0.0540	147.
6	0.0687	122.	0.0550	147.

Table 2.2: Steady-state responses, examples 3,4

Node	<i>Example 5, $c = 0.02k_s$</i>		<i>Example 6, $c = 0.05k_s$</i>	
	Amplitude, <i>mm</i>	Phase angle, $^\circ$	Amplitude, <i>mm</i>	Phase angle, $^\circ$
1	0.0253	186.	0.0243	193.
2	0.0221	179.	0.0229	176.
3	0.0241	178.	0.0249	175.
4	0.0232	186.	0.0222	194.
5	0.0499	162.	0.0489	173.
6	0.0509	162.	0.0499	172.

Table 2.3: Steady-state responses, examples 5,6

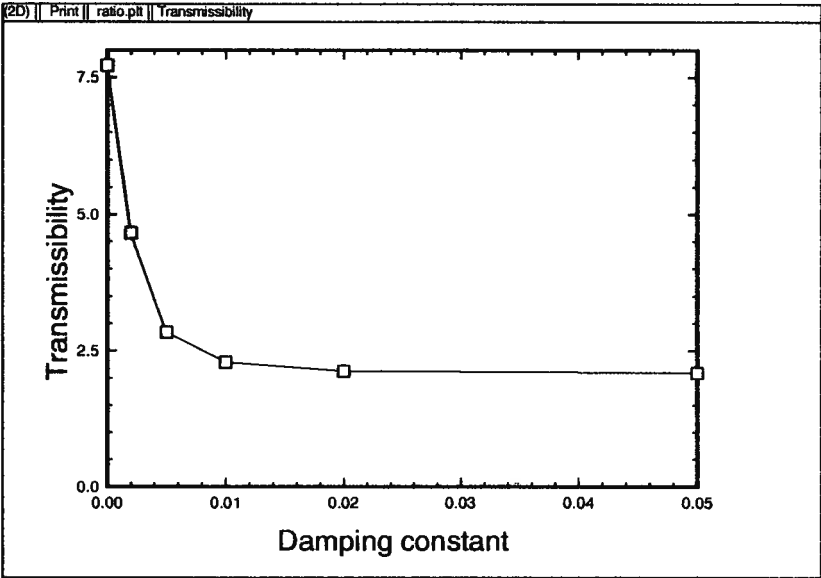


Figure 2.7: Effect of damping on transmissibility

Chapter 3

Formulation of component mode synthesis method

3.1 Undamped systems

In this chapter, the formulation of CMS method developed in this study will be presented for the case of undamped systems (in this section) and nonclassically damped systems in section 3.2. This formulation will be shown on an example of a two component system and the case of an arbitrary number of components will be considered in section 3.3.

The component mode synthesis method is a procedure in which the exact solution is approximated by one constructed from some basis vectors (e.g., mode shapes) of subsystems (components of subdivided system). This method allows a significant reduction of the eigenvalue equation size due to the use of a limited number of basis vectors. The approximate solution for the lower eigenvalues and eigenvectors is very close to the exact one due to the proper selection of the basis vectors and the use of Galerkin's method that determines the best approximation.

Consider a system subdivided into two adjacent components (call them the 1st and the 2nd) with interface S (Fig.3.1). The equation of free motion of the system in a natural mode $X(t) = e^{i\omega t} \phi$ with frequency ω and eigenvector $\phi = [\phi_1 \ \phi_2]^T$ can be written in the following form:

$$\left(-\omega^2 \begin{bmatrix} m_1 & 0 \\ 0 & m_2 \end{bmatrix} + \begin{bmatrix} k_1 & 0 \\ 0 & k_2 \end{bmatrix} \right) \begin{bmatrix} \phi_1 \\ \phi_2 \end{bmatrix} = \begin{bmatrix} f_1 \\ f_2 \end{bmatrix} \quad (3.1)$$

where term $e^{i\omega t}$ was cancelled, m_1, m_2 are the mass matrices of the components and

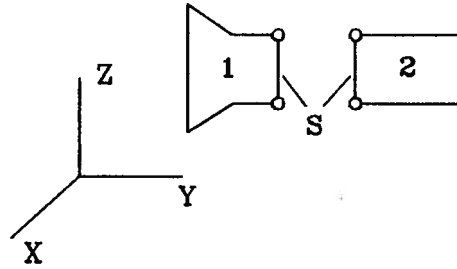


Figure 3.1: Two component system

k_1, k_2 the stiffness matrices. The force vectors f_1, f_2 will contain only interface forces (interaction between components), which appear as external forces at the artificial subdivision of the system and all the remaining components of f_1, f_2 corresponding to the component internal degrees of freedom will be zero, because of the absence of external forces. As can be noted the system eigenvector was also subdivided into two subvectors ϕ_1, ϕ_2 corresponding to the 1st and 2nd components. Rewrite (3.1) in the abbreviated form:

$$(-\omega^2 \hat{M} + \hat{K})\phi = f \quad (3.2)$$

Subvectors ϕ_1, ϕ_2 will be approximated in the following form:

$$\phi_1 \approx \tilde{\phi}_1 = \begin{bmatrix} \Phi_1^l & \Phi_1^a \end{bmatrix} \begin{bmatrix} p_1^l \\ p_1^a \end{bmatrix} \quad (3.3)$$

$$\phi_2 \approx \tilde{\phi}_2 = \begin{bmatrix} \Phi_2^l & \Phi_2^a \end{bmatrix} \begin{bmatrix} p_2^l \\ p_2^a \end{bmatrix} \quad (3.4)$$

where $\Phi_1^l, \Phi_2^l =$ matrices of lower (retained) free-free vibration modes (including rigid-body modes) for 1st and 2nd components respectively (determined as the result of eigenproblem solution for free-free component), $\Phi_1^a, \Phi_2^a =$ matrices of residual-attachment modes for 1st and 2nd components, p_1^l, p_2^l vectors of free-free mode coordinates for 1st

and 2nd components, p_1^a , p_2^a vectors of residual-attachment modes mode coordinates for 1st and 2nd components.

Consider the determination of residual-attachment modes. Take the 1st component equation from (3.1)

$$(-\omega^2 m_1 + k_1) \phi_1 = f_1$$

Use the transformation to modal coordinates $\phi_1 = \Phi_1 p_1$ ($\Phi_1 =$ complete set of free-free mass-normalized modes of the 1st component) and premultiplying by Φ_1^T one can obtain:

$$\left(\omega^2 \begin{bmatrix} I & 0 \\ 0 & I \end{bmatrix} + \begin{bmatrix} \omega_{l1}^2 & 0 \\ 0 & \omega_{h1}^2 \end{bmatrix} \right) \begin{bmatrix} p_{l1} \\ p_{h1} \end{bmatrix} = \begin{bmatrix} \Phi_{l1}^T \\ \Phi_{h1}^T \end{bmatrix} f_1 \quad (3.5)$$

where Φ_1 was partitioned into two sets Φ_{l1} , Φ_{h1} (index l means lower (retained) modes, $h =$ higher modes of component), ω_{l1}^2 , $\omega_{h1}^2 =$ diagonal matrices with natural component frequencies squared.

The assignment of the number of retained modes for each component will depend on the range of system frequencies, which are supposed to be evaluated by an application of this method. It may be seen from (3.5) that if

$$\omega^2 \ll \min[\omega_{h1}^2] \quad (3.6)$$

then the approximate expression for the modal coordinates p_{h1} follows [10], [30]:

$$p_{h1} \approx [\omega_{h1}^2]^{-1} \Phi_{h1}^T f_1$$

Thus the contribution of the higher modes to the subvector ϕ_1 can be approximated as

$$\Phi_{h1} p_{h1} \approx \Phi_{h1} [\omega_{h1}^2]^{-1} \Phi_{h1}^T f_1 \quad (3.7)$$

where the columns of matrix $R_1 = \Phi_{h1} [\omega_{h1}^2]^{-1} \Phi_{h1}^T$ corresponding to the interface degrees of freedom are called residual-attachment modes. Due to (3.7) the interface forces in f_1 will be identified with the residual-attachment mode coordinates p_1^a .

The number of retained free-free component modes should be high enough, in order that condition (3.6) and consequently expression (3.7) are satisfied at the proper level, such that a good approximation for the subvector ϕ_1 by means of the basis vectors Φ_1^l and Φ_1^a (the selected columns of matrices Φ_1 , R_1 respectively) will be obtained. The matrix R_1 can be expressed in an advantageous form [10], [30], [4]:

$$R_1 = k_1^{-1} - \Phi_{l1}[\omega_{l1}^2]^{-1}\Phi_{l1}^T$$

This means that computation of the lower modes only is required for each component, which leads to economy of computer time. In the case of an unconstrained component, inversion of the stiffness matrix will be considered below. An analogous determination of residual-attachment modes is conducted for the second component.

Thus combining (3.3), (3.4) the system eigenvector is approximated as

$$\phi \approx \tilde{\phi} = \begin{bmatrix} \tilde{\phi}_1 \\ \tilde{\phi}_2 \end{bmatrix} = \begin{bmatrix} \Phi_1^l & \Phi_1^a & 0 & 0 \\ 0 & 0 & \Phi_2^l & \Phi_2^a \end{bmatrix} \begin{bmatrix} p_1^l \\ p_1^a \\ p_2^l \\ p_2^a \end{bmatrix}$$

or in abbreviated form

$$\tilde{\phi} = \hat{\Phi}p \quad (3.8)$$

Imposing the condition of force continuity at the interface nodes gives:

$$p_1^a = -p_2^a \quad (3.9)$$

Using (3.9) one can express the vector p through a vector q' , which will not contain p_2^a :

$$\begin{bmatrix} p_1^l \\ p_1^a \\ p_2^l \\ p_2^a \end{bmatrix} = \begin{bmatrix} I & 0 & 0 \\ 0 & I & 0 \\ 0 & 0 & I \\ 0 & -I & 0 \end{bmatrix} \begin{bmatrix} p_1^l \\ p_1^a \\ p_2^l \end{bmatrix} \quad (3.10)$$

or in abbreviated form

$$p = \beta' q'$$

Subvectors $\tilde{\phi}_1$ and $\tilde{\phi}_2$ can be written in the following form:

$$\tilde{\phi}_1 = \begin{bmatrix} \tilde{\phi}_1^B \\ \tilde{\phi}_1^i \end{bmatrix} = \begin{bmatrix} \Phi_{1B}^l & \Phi_{1B}^a \\ \Phi_{1i}^l & \Phi_{1i}^a \end{bmatrix} \begin{bmatrix} p_1^l \\ p_1^a \end{bmatrix}$$

and

$$\tilde{\phi}_2 = \begin{bmatrix} \tilde{\phi}_2^B \\ \tilde{\phi}_2^i \end{bmatrix} = \begin{bmatrix} \Phi_{2B}^l & \Phi_{2B}^a \\ \Phi_{2i}^l & \Phi_{2i}^a \end{bmatrix} \begin{bmatrix} p_2^l \\ -p_1^a \end{bmatrix}$$

where $\tilde{\phi}^B$ = displacements at the interface, $\tilde{\phi}^i$ all the remaining displacements. Apply the equation of continuity of displacements at the interface:

$$\tilde{\phi}_1^B = \tilde{\phi}_2^B \quad (3.11)$$

thus it follows from the above expressions that

$$\Phi_{1B}^l p_1^l + \Phi_{1B}^a p_1^a = \Phi_{2B}^l p_2^l - \Phi_{2B}^a p_1^a$$

Therefore one can express the interface forces in terms of free-free mode coordinates:

$$p_1^a = \begin{bmatrix} T_1 & T_2 \end{bmatrix} \begin{bmatrix} p_1^l \\ p_2^l \end{bmatrix}$$

where

$$T_1 = (\Phi_{1B}^a + \Phi_{2B}^a)^{-1}(-\Phi_{1B}^l)$$

$$T_2 = (\Phi_{1B}^a + \Phi_{2B}^a)^{-1}(\Phi_{2B}^l)$$

Thus the following relation will hold:

$$\begin{bmatrix} p_1^l \\ p_1^a \\ p_2^l \end{bmatrix} = \begin{bmatrix} I & 0 \\ T_1 & T_2 \\ 0 & I \end{bmatrix} \begin{bmatrix} p_1^l \\ p_2^l \end{bmatrix} \quad (3.12)$$

or in the abbreviated form:

$$q' = \beta'' q$$

Therefore the vector p of all generalized coordinates can be expressed in terms of independent generalized coordinates $q = [p_1^t \ p_2^t]^T$:

$$p = \beta' \beta'' q$$

or

$$p = \beta q \tag{3.13}$$

where $\beta = \beta' \beta''$.

Substituting (3.13) in (3.8) the relation between the approximate system eigenvector and vector q will be:

$$\tilde{\phi} = \hat{\Phi} \beta q \tag{3.14}$$

Substituting (3.14) in (3.2) one can obtain:

$$(-\omega^2 \hat{M} + \hat{K}) \hat{\Phi} \beta q = f + \epsilon$$

where the quantity ϵ represents an approximation error. Galerkin's method (premultiplying ϵ by basis functions and setting it to zero) yields the following matrix equation

$$\beta^T \hat{\Phi}^T (-\omega^2 \hat{M} + \hat{K}) \hat{\Phi} \beta q = \beta^T \hat{\Phi}^T f \tag{3.15}$$

and the vector on the right side vanishes in the absence of external forces. This fact is due to the equal displacements and opposite forces at the interface. To show it consider the product of an arbitrary vector q and vector $\beta^T \hat{\Phi}^T f$, namely,

$$q^T \beta^T \hat{\Phi}^T f = \begin{bmatrix} \tilde{\phi}_1^T & \tilde{\phi}_2^T \end{bmatrix} \begin{bmatrix} f_1 \\ f_2 \end{bmatrix}$$

and if only interface forces are present, then the above expression is transformed to the following one:

$$[\tilde{\phi}_1^B]^T [p_1^a] + [\tilde{\phi}_2^B]^T [p_2^a]$$

Taking into account the (3.11) and (3.9) the above expression becomes a zero vector. Therefore the product of vectors q and $\beta^T \hat{\Phi}^T f$ is always zero for an arbitrary vector q , which means that vector $\beta^T \hat{\Phi}^T f$ must be zero and the right side of equation (3.15) vanishes.

Thus the final condensed equation of motion for two coupled components (or the whole system) in terms of generalized coordinates can be written in the following form:

$$(-\omega^2 M_* + K_*)q = 0$$

where $M_* = \beta^T \hat{\Phi}^T \hat{M} \hat{\Phi} \beta$, $K_* = \beta^T \hat{\Phi}^T \hat{K} \hat{\Phi} \beta$ will be real symmetric matrices. This equation represents an eigenvalue problem. The eigenvalues ω^2 and eigenvectors q will be all real quantities.

3.1.1 Case of an unconstrained component. Method of weak springs

A new approach to treat an unconstrained component is developed by imposing "weak" constraints (springs) on the system, which remove the singularity of the stiffness matrix and make it invertible. The stiffness of "weak" springs can be assumed to be $10^{-7} k_{ii}$, where k_{ii} are corresponding diagonal elements of the stiffness matrix, which are supposed to be modified. If a smaller value is chosen the modified stiffness matrix may not be invertible (the numerical aspect of inversion should be taken into account). This method requires less computational effort than the method described in [27]. The lowest (strictly speaking non-zero, but near zero) frequencies will correspond to the rigid-body modes. These rigid-body modes will be strictly speaking "flexible" modes due to the introduced

"weak" springs, but the stiffnesses of these "weak" springs should be negligible compared to the component and system stiffnesses, so these "flexible" modes will actually correspond to the motions of the component as a rigid body.

To illustrate this method consider the example of an unconstrained component such as a linear bar element (Fig.3.2), which can move along the X axis. The bar element has two degrees of freedom x_1 , x_2 and the corresponding stiffness matrix is

$$k = \frac{EA}{L} \begin{bmatrix} 1 & -1 \\ -1 & 1 \end{bmatrix}$$

where E = modulus of elasticity, A = cross-section area, L = length of the element. The determinant of k equals 0. The mass matrix has the following form:

$$m = \frac{\rho AL}{6} \begin{bmatrix} 2 & 1 \\ 1 & 2 \end{bmatrix}$$

where ρ = density of material. The eigensolution will yield:

$$\lambda_1 = 0, \quad \phi_1 = [a, a] \quad (\text{rigid - body mode})$$

$$\lambda_2 = 2\eta, \quad \phi_2 = [a, -a] \quad (\text{flexible mode})$$

where $\eta = 6\frac{E}{\rho L^2}$.

Introduce a weak spring with stiffness $= \epsilon\frac{EA}{L}$, attached to one of the nodes (Fig.3.2), then the stiffness matrix becomes invertible

$$k' = \frac{EA}{L} \begin{bmatrix} 1 + \epsilon & -1 \\ -1 & 1 \end{bmatrix}$$



Figure 3.2: Linear bar element

If $\epsilon = 0.001$, then the eigensolution will yield:

$$\lambda_1 = 0.00016\eta, \quad \phi_1 = [a, 1.0005a] \quad (\text{"rigid - body" mode})$$

$$\lambda_2 = 2.0005\eta, \quad \phi_2 = [a, -0.99983a] \quad (\text{flexible mode})$$

The approximation error for eigenvalues and eigenvectors is less than 0.05%. Therefore an unconstrained component can be modelled as constrained if ϵ is small enough.

3.2 Nonclassically damped systems

In this section the formulation shown in section 3.1 is generalized to nonclassically damped systems, using state-space representation.

Consider again a system subdivided into two adjacent components with interface S (Fig.3.1). The equation of free motion of the system subdivided into two components will have the following form:

$$\begin{bmatrix} m_1 & 0 \\ 0 & m_2 \end{bmatrix} \begin{bmatrix} \ddot{U}_1 \\ \ddot{U}_2 \end{bmatrix} + \begin{bmatrix} c_1 & 0 \\ 0 & c_2 \end{bmatrix} \begin{bmatrix} \dot{U}_1 \\ \dot{U}_2 \end{bmatrix} + \begin{bmatrix} k_1 & 0 \\ 0 & k_2 \end{bmatrix} \begin{bmatrix} U_1 \\ U_2 \end{bmatrix} = \begin{bmatrix} f_1(t) \\ f_2(t) \end{bmatrix}$$

where U_1, U_2 are displacement vectors of the 1st and 2nd components respectively.

The state-space representation reduces this equation to the following one:

$$\hat{A}\dot{Y} + \hat{B}Y = F_c(t)$$

where

$$\hat{A} = \begin{bmatrix} A_1 & 0 \\ 0 & A_2 \end{bmatrix}, \hat{B} = \begin{bmatrix} B_1 & 0 \\ 0 & B_2 \end{bmatrix}, Y = \begin{bmatrix} Y_1 \\ Y_2 \end{bmatrix}, F_c = \begin{bmatrix} F_1 \\ F_2 \end{bmatrix},$$

$$A_1 = \begin{bmatrix} c_1 & m_1 \\ m_1 & 0 \end{bmatrix}, A_2 = \begin{bmatrix} c_2 & m_2 \\ m_2 & 0 \end{bmatrix}, B_1 = \begin{bmatrix} k_1 & 0 \\ 0 & -m_1 \end{bmatrix}, B_2 = \begin{bmatrix} k_2 & 0 \\ 0 & -m_2 \end{bmatrix},$$

$$Y_1 = \begin{bmatrix} U_1 \\ \dot{U}_1 \end{bmatrix}, Y_2 = \begin{bmatrix} U_2 \\ \dot{U}_2 \end{bmatrix}, F_1 = \begin{bmatrix} f_1 \\ 0 \end{bmatrix}, F_2 = \begin{bmatrix} f_2 \\ 0 \end{bmatrix}$$

The equation of free motion of the system in a system mode $Y = e^{\lambda t}\phi$ with system eigenvalue λ and system state-space eigenvector $\phi = [\phi_1 \ \phi_2]^T$ (subdivided also) will have the following form:

$$\left(\lambda \begin{bmatrix} A_1 & 0 \\ 0 & A_2 \end{bmatrix} + \begin{bmatrix} B_1 & 0 \\ 0 & B_2 \end{bmatrix} \right) \begin{bmatrix} \phi_1 \\ \phi_2 \end{bmatrix} = \begin{bmatrix} F_{1*} \\ F_{2*} \end{bmatrix} \quad (3.16)$$

or in the abbreviated form:

$$(\lambda \hat{A} + \hat{B})\phi = F_{\star} \quad (3.17)$$

where F_{\star} is defined by the equation:

$$F_c = F_{\star} e^{\lambda t}$$

The force vectors $F_{1\star}$, $F_{2\star}$ will contain only interface forces (interaction between components) which appear as external forces at the artificial subdivision of the system and all the remaining components of $F_{1\star}$, $F_{2\star}$ corresponding to the component internal degrees of freedom will be zero, because of the absence of external forces. In this state-space representation λ , ϕ , F_{\star} are assumed complex.

The complex subvectors ϕ_1 and ϕ_2 are approximated in the following form:

$$\phi_1 \approx \tilde{\phi}_1 = \begin{bmatrix} \Phi_1^l & \Phi_1^a \end{bmatrix} \begin{bmatrix} p_1^l \\ p_1^a \end{bmatrix} \quad (3.18)$$

$$\phi_2 \approx \tilde{\phi}_2 = \begin{bmatrix} \Phi_2^l & \Phi_2^a \end{bmatrix} \begin{bmatrix} p_2^l \\ p_2^a \end{bmatrix} \quad (3.19)$$

where free-free vibration modes Φ_1^l , Φ_2^l are complex and a complex eigensolver is used to compute them. Note the modal coordinates p^l , p^a are also complex in general.

Consider the determination of residual-attachment modes Φ_1^a , Φ_2^a . Take the 1st component equation from (3.16)

$$(\lambda A_1 + B_1)\phi_1 = F_{1\star}$$

Use the transformation to modal coordinates $\phi_1 = \Phi_1 p_1$ (Φ_1 = complete set of free-free A-normalized modes of the 1st component) and premultiplying by Φ_1^T one can obtain:

$$\left(\lambda \begin{bmatrix} I & 0 \\ 0 & I \end{bmatrix} + \begin{bmatrix} \lambda_{l1} & 0 \\ 0 & \lambda_{h1} \end{bmatrix} \right) \begin{bmatrix} p_{l1} \\ p_{h1} \end{bmatrix} = \begin{bmatrix} \Phi_{l1}^T \\ \Phi_{h1}^T \end{bmatrix} F_{1\star} \quad (3.20)$$

where Φ_1 was partitioned into two sets Φ_{l1} , Φ_{h1} (index l means lower (retained) modes, h = higher modes of component), λ_{l1} , λ_{h1} = diagonal matrices with component eigenvalues.

The assignment of the number of retained modes for each component will depend on the range of system eigenvalues, which are supposed to be evaluated by an application of this method. It may be seen from (3.20) that if

$$|\lambda| \ll \min[|\lambda_{h1}|] \quad (3.21)$$

then the approximate expression for the modal coordinates p_{h1} follows

$$p_{h1} \approx [\lambda_{h1}]^{-1} \Phi_{h1}^T F_{1*}$$

Thus the contribution of the higher modes to the subvector ϕ_1 can be approximated as

$$\Phi_{h1} p_{h1} \approx \Phi_{h1} [\lambda_{h1}]^{-1} \Phi_{h1}^T F_{1*} \quad (3.22)$$

where the columns of matrix $R_1 = \Phi_{h1} [\lambda_{h1}]^{-1} \Phi_{h1}^T$ corresponding to the interface degrees of freedom will be called state-space residual-attachment modes, which will be complex in this case. Due to (3.22) the interface forces in F_{1*} will be identified with the residual-attachment mode coordinates p_1^a .

The number of retained component modes should be high enough, in order that condition (3.21) and consequently expression (3.22) are satisfied at the proper level, such that a good approximation for the subvector ϕ_1 by means of basis vectors Φ_1^l , Φ_1^a (the selected columns of matrices Φ_1 , R_1 respectively) will be obtained.

The matrix R_1 can be expressed in the following form:

$$R_1 = B_1^{-1} - \Phi_{l1} [\lambda_{l1}]^{-1} \Phi_{l1}^T$$

This means that computation of the lower eigenvectors only is required for each component, which leads to economy of computer time. The inversion of matrix B_1 is determined

by independent inversion of matrices m_1, k_1 . In the case of an unconstrained component the inversion of the stiffness matrix was discussed before. An analogous determination of residual-attachment modes is conducted for the second component.

Thus combining (3.18), (3.19) the system eigenvector is approximated as

$$\phi \approx \tilde{\phi} = \begin{bmatrix} \tilde{\phi}_1 \\ \tilde{\phi}_2 \end{bmatrix} = \begin{bmatrix} \Phi_1^l & \Phi_1^a & 0 & 0 \\ 0 & 0 & \Phi_2^l & \Phi_2^a \end{bmatrix} \begin{bmatrix} p_1^l \\ p_1^a \\ p_2^l \\ p_2^a \end{bmatrix}$$

or in abbreviated form

$$\tilde{\phi} = \hat{\Phi} p \quad (3.23)$$

Apply the equation of force continuity at the interface:

$$p_1^a = -p_2^a \quad (3.24)$$

Equation (3.24) is used to eliminate the attachment mode coordinates p_2^a from the generalized coordinate vector p , i.e., using a matrix transformation (see analogous transformation (3.10)) one can obtain:

$$p = \beta' q' \quad (3.25)$$

where vector q' does not contain coordinates p_2^a .

The subvectors $\tilde{\phi}_1, \tilde{\phi}_2$ can be partitioned in the following way:

$$\tilde{\phi}_1 = \begin{bmatrix} \tilde{\phi}_1^B \\ \tilde{\phi}_1^i \end{bmatrix}$$

and

$$\tilde{\phi}_2 = \begin{bmatrix} \tilde{\phi}_2^B \\ \tilde{\phi}_2^i \end{bmatrix}$$

where $\tilde{\phi}^B$ = displacements at the interface, $\tilde{\phi}^i$ = all the remaining displacements. Apply the equation of displacement continuity at the interface:

$$\tilde{\phi}_1^B = \tilde{\phi}_2^B \quad (3.26)$$

Expression (3.26) is used to eliminate residual-attachment mode coordinates from the vector q' expressing them in terms of free-free mode coordinates, i.e, using a matrix transformation (see analogous transformation (3.12)) one can obtain:

$$q' = \beta'' q \quad (3.27)$$

where the vector

$$q = \begin{bmatrix} p_1^l \\ p_2^l \end{bmatrix}$$

Substituting (3.27) in (3.25) the vector p of all generalized coordinates is expressed in terms of independent generalized coordinates q :

$$p = \beta' \beta'' q$$

or

$$p = \beta q \quad (3.28)$$

where $\beta = \beta' \beta''$.

Substituting (3.28) in (3.23) the relation between the approximate system eigenvector $\tilde{\phi}$ and the vector of generalized coordinates q will be

$$\tilde{\phi} = \hat{\Phi} \beta q \quad (3.29)$$

Substitution of (3.29) in (3.17) gives:

$$(\lambda \hat{A} + \hat{B}) \hat{\Phi} \beta q = F_* + \epsilon$$

where the quantity ϵ represents an approximation error. Galerkin's method again yields the following matrix equation:

$$\beta^T \hat{\Phi}^T (\lambda \hat{A} + \hat{B}) \hat{\Phi} \beta q = \beta^T \hat{\Phi}^T F_*$$

and the vector on the right side vanishes (it was proved in section 3.1).

Therefore the final condensed equation of motion in a system mode for two coupled components (or the whole system) in terms of generalized coordinates can be written as:

$$(\lambda A_* + B_*)q = 0$$

where $A_* = \beta^T \hat{\Phi}^T \hat{A} \hat{\Phi} \beta$, $B_* = \beta^T \hat{\Phi}^T \hat{B} \hat{\Phi} \beta$ will be complex symmetric matrices.

The solution of this eigenvalue equation yields the complex conjugate eigenvalues λ and eigenvectors q in general. There may be an even number of real eigenvalues, which will correspond to overdamped modes (depending upon the damping properties of the system). In the case when c_1, c_2 are zero matrices (undamped system) the eigenvalues will be pure imaginary (zero real parts).

3.2.1 Component mode selection procedure

Selection of lower (retained) modes is made on the basis of the absolute values of the eigenvalues which are complex numbers. Thus both the imaginary part (frequency) and the real part of the eigenvalue are counted. This will be important when a component is heavily damped. In the case of an undamped component, selection of retained modes will be based on the lower frequencies (imaginary parts), because the real parts of the eigenvalues are zeros.

The ratio

$$r = \frac{|\lambda_{com}|}{|\lambda_{sys}|}$$

yields the boundary separating the lower (retained) and higher modes of a component, where λ_{sys} is the largest system eigenvalue of interest and λ_{com} is the boundary component eigenvalue out of the retained eigenvalues. This procedure can be illustrated as follows in Fig.3.3. The solid circle indicates the level of system eigenvalue of interest and the dashed one corresponds to the level of retained eigenvalues (eigenvectors) for each component. All the eigenvectors with eigenvalues located in sector D (within of dashed circle) will be retained modes, and all the eigenvalues beyond of this sector will correspond to the higher modes, which are not used in the analysis.

It has been established by conducting a series of numerical computations for different systems (including heavily damped systems) that a good accuracy for the given range $0 \Leftrightarrow |\lambda_{sys}|$ can be achieved with $r = 2$. Note that the greater r the better accuracy, but the larger the size of the condensed eigenproblem.

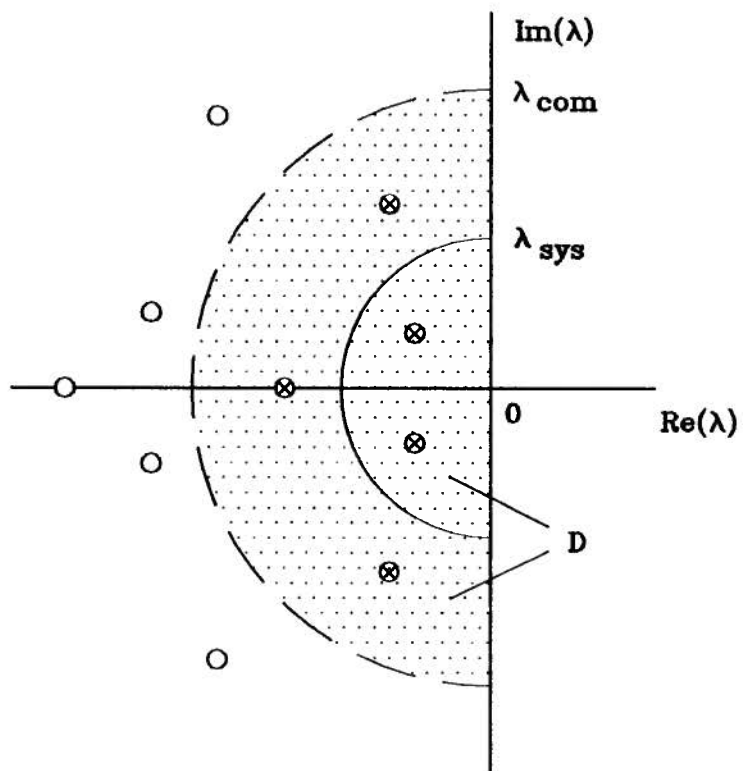


Figure 3.3: Mode selection procedure

3.3 Case of an arbitrary number of components

Generalization of the developed method (sections 3.1,3.2) to a system with an arbitrary number of components is straightforward and shown here only in a brief form. This generalization is conducted simultaneously for the both cases: undamped and nonclassically damped system.

Consider a system consisting of N components, which are joined by L interfaces. Consider the j th interface, which identifies two adjacent components (call them the 1st and 2nd one). Introduce the following notations:

$$\hat{p}_1^a = \left[p_{11}^a \quad p_{12}^a \quad \dots \quad p_{1j}^a \quad \dots \quad p_{1L}^a \right]^T$$

and

$$\hat{p}_2^a = \left[p_{21}^a \quad p_{22}^a \quad \dots \quad p_{2j}^a \quad \dots \quad p_{2L}^a \right]^T$$

where vectors \hat{p}_1^a and \hat{p}_2^a consist of interface force vectors of all interfaces. Apply the equation of force equilibrium at the j th interface:

$$p_{1j}^a = -p_{2j}^a \quad j = 1, 2, \dots, L \quad (3.30)$$

Using (3.30) one can express the vector of generalized coordinates p (see analogous matrix transformation (3.10)) through the vector q' , which will not contain \hat{p}_2^a :

$$p = \beta' q'$$

Consider now the displacements at the j th interface $\tilde{\phi}_{1j}^B$ and $\tilde{\phi}_{2j}^B$. These subvectors $\tilde{\phi}_{1j}^B$ and $\tilde{\phi}_{2j}^B$ can be expressed in the following form:

$$\tilde{\phi}_{1j}^B = \Phi_{1B}^l p_1^l + \Phi_{1B}^a \check{p}_1^a \quad \tilde{\phi}_{2j}^B = \Phi_{2B}^l p_2^l + \Phi_{2B}^a \check{p}_2^a \quad j = 1, 2, \dots, L$$

where the vectors \check{p}_1^a , \check{p}_2^a combine all the interface force vectors, which belong to the components 1 and 2 respectively:

$$\check{p}_1^a = \left[p_{1i}^a \quad \dots \quad p_{1k}^a \right]^T$$

and

$$\tilde{p}_2^a = \begin{bmatrix} p_{1l}^a & \dots & p_{1n}^a \end{bmatrix}^T$$

where $i, \dots, k =$ numbers of the interfaces, which belong to component 1 and l, \dots, n to component 2.

The compatibility of displacements at the j th interface yields the following system of equations

$$\tilde{\phi}_{1j}^B = \tilde{\phi}_{2j}^B \quad j = 1, 2, \dots, L$$

which can be used to express the interface forces p_{1j}^a ($j = 1, 2, \dots, L$) in terms of free-free mode coordinates. Thus the vector q' can be expressed (see analogous transformation (3.12)) by the following matrix transformation:

$$q' = \beta'' q$$

where

$$q = \begin{bmatrix} p_1^i & \dots & p_i^i & \dots & p_N^i \end{bmatrix}^T$$

and p_i^i is a set of free-free mode coordinates for the i th component. Therefore the vector of all generalized coordinates p is expressed in terms of independent generalized coordinates q in the following matrix transformation:

$$p = \beta' \beta'' q$$

or

$$p = \beta q$$

where $\beta = \beta' \beta''$.

Thus the relation between the approximate system eigenvector $\tilde{\phi}$ and the vector of independent generalized coordinates q will be

$$\tilde{\phi} = \hat{\Phi} \beta q$$

Analogous manipulations (see sections 3.1,3.2) with the equation of free motion of the subdivided system will yield the final condensed eigenproblems in terms of generalized coordinates. For the case of an undamped system:

$$(-\omega^2 M_* + K_*)q = 0$$

where $M_* = \beta^T \hat{\Phi}^T \hat{M} \hat{\Phi} \beta$, $K_* = \beta^T \hat{\Phi}^T \hat{K} \hat{\Phi} \beta$ will be real symmetric matrices. For a damped system:

$$(\lambda A_* + B_*)q = 0$$

where $A_* = \beta^T \hat{\Phi}^T \hat{A} \hat{\Phi} \beta$, $B_* = \beta^T \hat{\Phi}^T \hat{B} \hat{\Phi} \beta$ will be complex symmetric matrices.

Chapter 4

Numerical results

4.1 Comparison of CMSFR method with "VAST" program for undamped systems

Comparison of the results obtained by the program using CMSFR method with the results obtained by the finite element program "VAST" [31] are shown in Tables 4.1-4.4. Note that the "VAST" analysis treated each system as a whole (without a component subdivision). The user's manual for the CMSFR program is presented in Appendix A. Below numerical results are shown for some examples of undamped systems (Fig.4.1, a-d), which are shown in subdivided form.

The geometric and physical parameters of the systems shown are as follows: in examples a) and b) the cross-section of beam and bar elements was $1 \times 1 \text{ m}$, in examples c) and d) $0.02 \times 0.02 \text{ m}$. The dimensions of the beam and bar element components within each example were the same and are shown in metres. The thickness of the membrane element (2nd component) in example c) is 0.02 m . In example d) the second component is represented by a brick element with parameters of a cube. The material of all elements is steel. For examples a),b),c) the motion is considered in the plane of the drawing. For example d) 3-D motion is considered.

The total number of retained modes for example a) was 20, which determines the size of the condensed eigenvalue problem (Table 4.1). This total number of the retained modes was composed of $4 + 6 + 6 + 4$ respectively for each component.

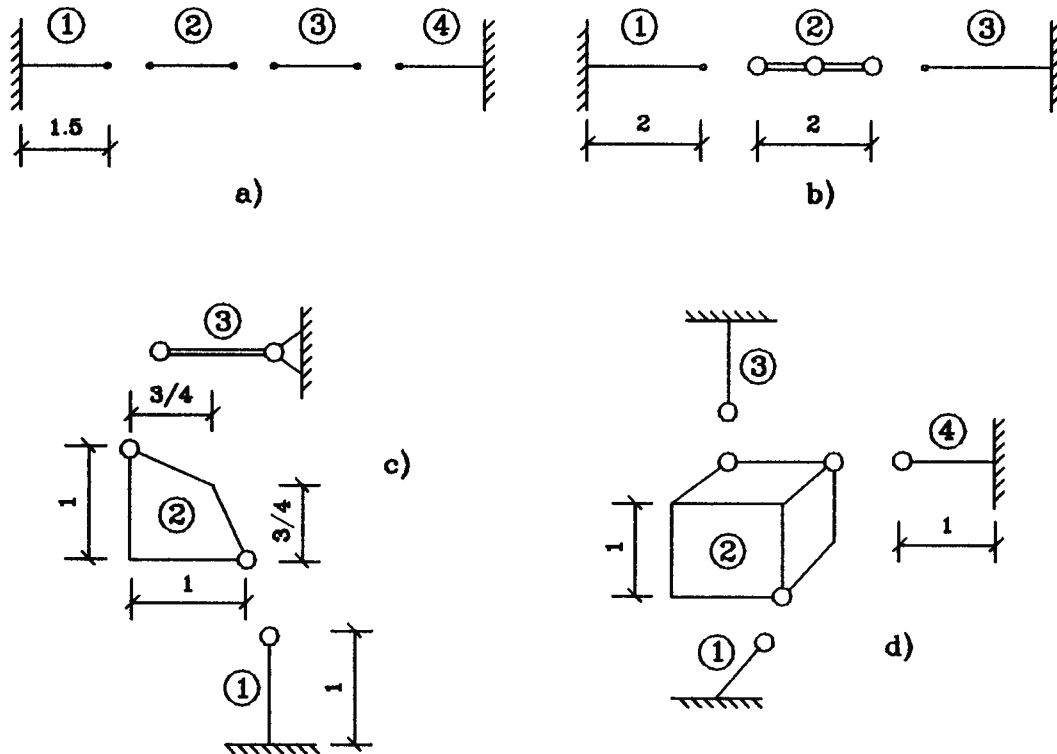


Figure 4.1: Test examples

A rigid-body mode exists for the system in Figure 4.1,b (Table 4.2), which was detected by the appearance of a low (near zero) frequency (the method of weak springs was used to treat unconstrained components). This system has bar elements in the 2nd component, that provides a rotational rigid-body degree of freedom at the joint of the bar elements. The current version of "VAST" does not detect such "hidden" rigid-body modes, because it has no algorithmic option to treat such systems.

The results for examples c), d) are presented in Tables 4.3, 4.4. Comparison of the 1st and 2nd mode shapes are shown in Fig.4.2,4.3 for the system in Fig.4.1,a. There is no difference between the modes calculated using CMSFR method and those calculated by "VAST" using the unsubdivided model.

<i>Frequencies, Hz</i>			
#	CMSFR	VAST	<i>Difference, %</i>
1	124.85	124.85	0.
2	298.25	298.25	0.
3	430.54	430.11	0.099
4	516.62	516.23	0.079
5	768.96	768.95	0.001
6	878.51	876.93	0.18
<i>Size of eigenvalue problem</i>			
CMSFR		VAST	
20 × 20		21 × 21	

Table 4.1: Four component beam element system: "a"

<i>Frequencies, Hz</i>			
#	CMSFR	VAST	<i>Difference, %</i>
1	0.044	-	-
2	140.35	140.35	0.
3	147.44	147.44	0.
3	432.89	432.28	0.14
4	633.57	633.48	0.014
5	643.38	643.30	0.012
6	898.45	894.15	0.48
<i>Size of eigenvalue problem</i>			
CMSFR		VAST	
11 × 11		14 × 14	

Table 4.2: Three component beam-bar element system with one rigid-body mode: "b"

<i>Frequencies, Hz</i>			
#	CMSFR	VAST	<i>Difference, %</i>
1	1.4666	1.4651	0.10
2	96.6478	96.660	0.012
3	126.485	126.46	0.019
4	313.73	313.73	0.
5	1979.3	1979.3	0.
<i>Size of eigenvalue problem</i>			
CMSFR		VAST	
12 × 12		9 × 9	

Table 4.3: Three component beam-bar-membrane element system: "c"

<i>Frequencies, Hz</i>			
#	CMSFR	VAST	<i>Difference, %</i>
1	0.2633	0.2631	0.076
2	0.3409	0.3409	0.
3	0.3664	0.3663	0.027
4	16.308	16.308	0.
5	38.242	38.228	0.036
6	38.255	38.241	0.036
<i>Size of eigenvalue problem</i>			
CMSFR		VAST	
12 × 12		33 × 33	

Table 4.4: Four component beam-brick element system: "d"

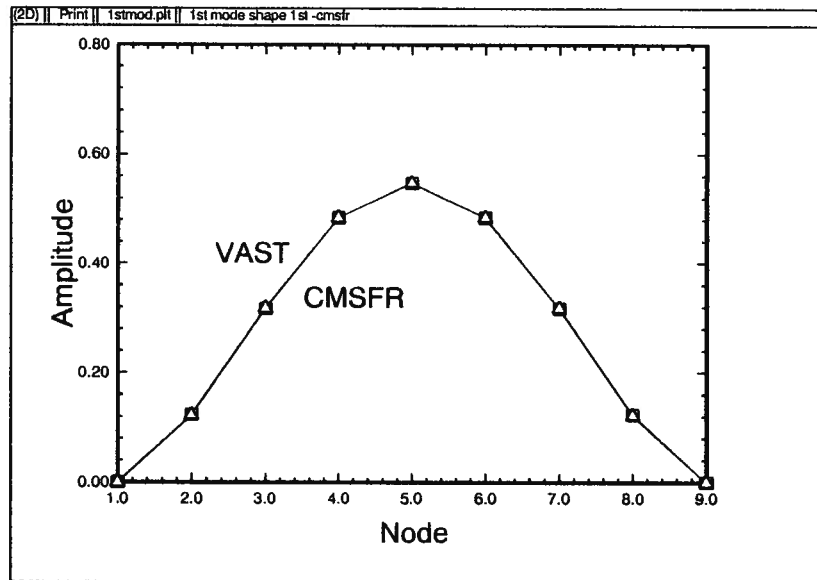


Figure 4.2: First mode shape of the system in Fig.4.1,a

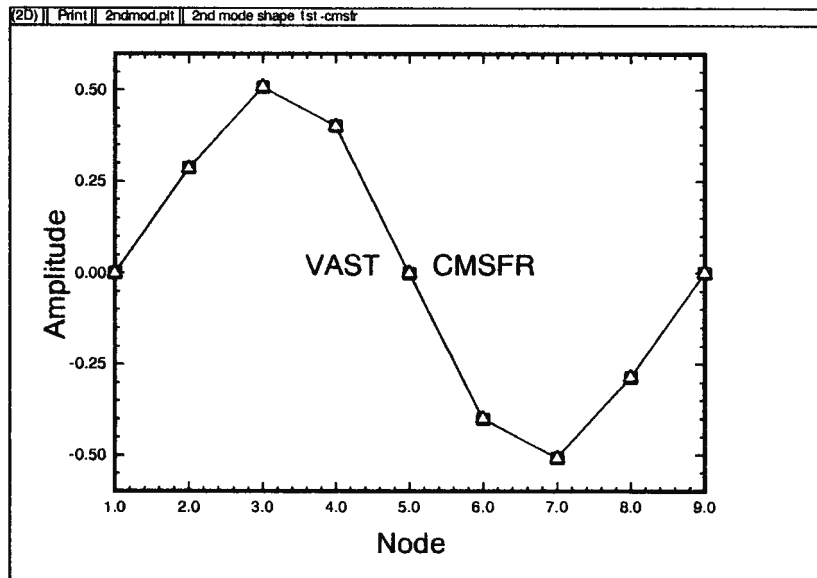


Figure 4.3: Second mode shape of the system in Fig.4.1,a

4.2 Comparison of CMSFR method with "DREIGN" program for undamped and nonclassically damped systems

Below some systems (without a component subdivision) are considered and their corresponding eigenvalue problems are solved by using a complex eigensolver "DREIGN" program [32], which uses the QR method. Then these results are compared with CMSFR method results for subdivided systems.

A two component system consisting of beam elements (Fig.4.4) was considered. The element cross-section was $0.01 \times 0.01 \text{ m}$. The damping matrices of the components were taken as stiffness-proportional ones on the component level, i.e., $c_1 = 0.00002k_1$, $c_2 = 0.00001k_2$, which produces nonclassical damping on the level of the whole system. The motion of the system is considered in the plane of the drawing. Table 4.5 presents a comparison of the results and shows excellent correspondence.

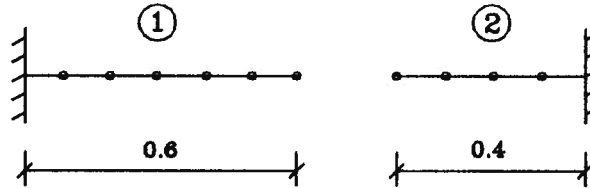


Figure 4.4: Two component beam element system

Then a three component system with lumped masses and dashpots was considered (Fig.4.5). The length of each component consisting of beam elements was 2 m , the cross-section of elements was $0.1 \times 0.1 \text{ m}$, the lumped masses were 100 kg each, the dashpots $10 \text{ N} \times \text{s/m}$ each. The motion of the system is considered in the plane of the drawing. The results are shown in Table 4.6.

Then two finite elements models of the vibration rig were considered (Fig.4.6). Parameters of the rig are shown in Appendix B. For application of the CMSFR method the finite element model of the rig was subdivided into four components (Fig.4.7). In

<i>Eigenvalues</i>						
	CMSFR		DREIGN		<i>Difference, %</i>	
#	Real, 1/s	Imag, Hz	Real, 1/s	Imag, Hz	Real	Imag
1	-0.8964	52.717	-0.8964	52.716	0.	0.
2	-6.396	145.34	-6.395	145.32	0.015	0.013
3	-26.303	285.06	-26.287	285.02	0.06	0.014
4	-70.22	472.73	-69.847	471.74	0.534	0.209
5	-157.15	707.65	-156.86	706.34	0.184	0.185
<i>Size of eigenvalue problem</i>						
	CMSFR		DREIGN			
	16 × 16 complex		54 × 54 real			

Table 4.5: Two component beam element system

the 1st model there were no damping elements present. Some damping properties were assumed for the elements a, b, c, d (Fig.4.7) for the 2nd model, producing an example of a nonclassically damped system. Comparison of the eigenvalues is presented in Tables 4.7, 4.9. Note that complex eigenvalues are obtained in pairs of conjugate numbers, but just one representative of each pair is shown in Tables 4.5-4.7,4.9. Good agreement between the results is obtained and a reduction of eigenvalue problem size is quite noticeable.

Comparison of the 1st eigenvectors for the undamped rig model is shown in Table 4.8. "Z" displacements of the 12 nodes (Fig. 4.8) were selected. The comparison of the 1st eigenvectors for the damped rig model is shown in Table 4.10.

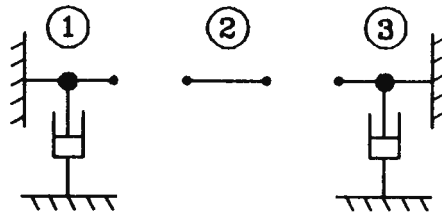


Figure 4.5: System with dashpots and lumped masses

<i>Eigenvalues</i>						
	CMSFR		DREIGN		<i>Difference, %</i>	
#	Real, 1/s	Imag, Hz	Real, 1/s	Imag, Hz	Real	Imag
1	-0.004433	14.044	-0.004433	14.044	0.	0.
2	-0.01609	33.699	-0.01609	33.698	0.	0.
3	-0.02204	60.588	-0.02204	60.588	0.	0.
4	-0.0140	101.94	-0.0140	101.89	0.	0.049
5	-0.005491	208.61	-0.005442	207.55	0.9	0.51
6	-0.001634	313.93	-0.001617	313.18	1.0	0.23
<i>Size of eigenvalue problem</i>						
CMSFR			DREIGN			
18 × 18 complex			24 × 24 real			

Table 4.6: System with dashpots and lumped masses

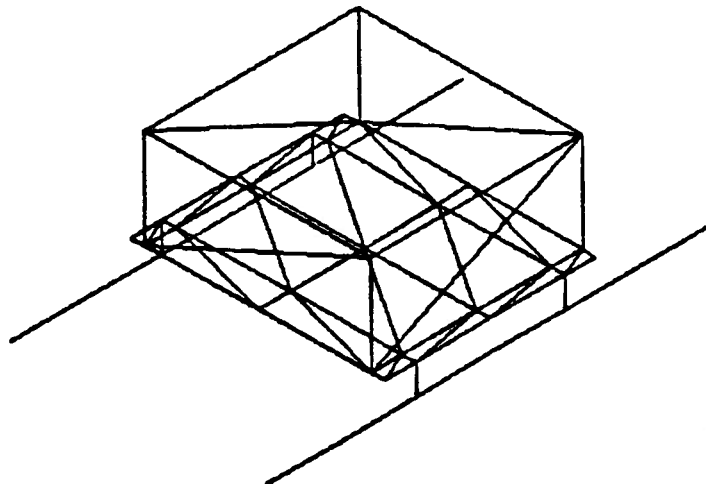


Figure 4.6: Finite element model of the rig

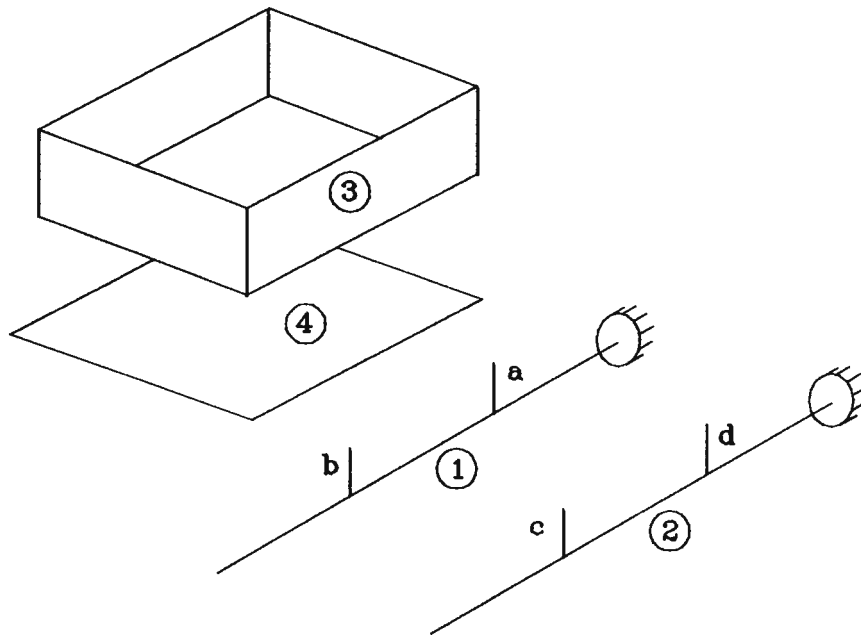


Figure 4.7: Four component presentation of the system

<i>Eigenvalues</i>					
	CMSFR		DREIGN		<i>Difference</i>
#	Real 1/s	Imag, Hz	Real 1/s	Imag, Hz	%
1	0.	4.791	0.	4.774	0.356
2	0.	5.767	0.	5.757	0.173
3	0.	6.121	0.	6.108	0.212
4	0.	8.144	0.	8.130	0.172
5	0.	8.357	0.	8.343	0.167
6	0.	9.212	0.	9.192	0.217
7	0.	31.46	0.	31.33	0.414
8	0.	31.57	0.	31.42	0.477
<i>Size of eigenvalue problem</i>					
CMSFR			DREIGN		
60 × 60 complex			516 × 516 real		

Table 4.7: Comparison of eigenvalues for the undamped rig model

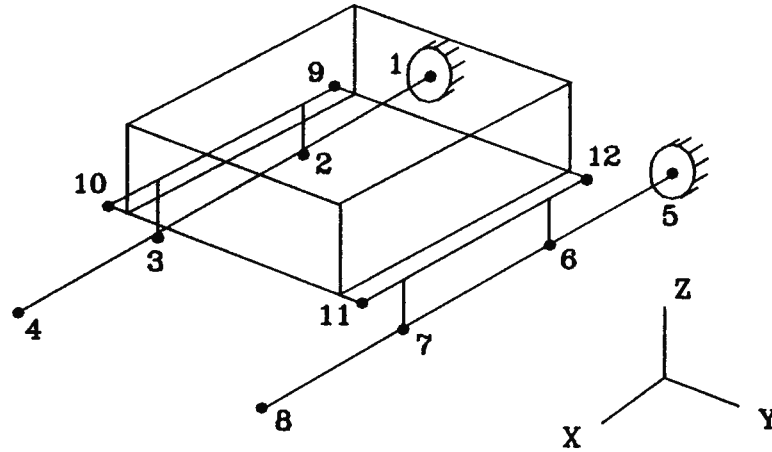


Figure 4.8: Selected nodes for the eigenvector presentation

<i>Z displacements in the 1st eigenvector</i>				
	CMSFR		DREIGN	
#	Real	Imag	Real	Imag
1	0.913E-06	-0.252E-11	0.105E-05	-0.443E-08
2	0.467E-01	0.000E+00	0.481E-01	-0.742E-04
3	0.134E+00	-0.378E-06	0.137E+00	-0.309E-03
4	0.229E+00	-0.882E-05	0.234E+00	-0.286E-03
5	0.104E-05	-0.136E-09	0.105E-05	-0.443E-08
6	0.481E-01	-0.189E-05	0.481E-01	-0.742E-04
7	0.137E+00	0.668E-05	0.137E+00	-0.309E-03
8	0.235E+00	-0.164E-04	0.234E+00	-0.286E-03
9	-0.643E+00	0.277E-04	-0.625E+00	0.578E-03
10	0.986E+00	-0.101E-04	0.100E+01	0.000E+00
11	0.100E+01	0.000E+00	0.100E+01	0.000E+00
12	-0.626E+00	-0.529E-04	-0.625E+00	0.578E-03

Table 4.8: Comparison of the 1st eigenvectors for the undamped rig model

<i>Eigenvalues</i>						
	CMSFR		DREIGN		<i>Difference</i>	
#	Real, 1/s	Imag, Hz	Real 1/s	Imag, Hz	Real, %	Imag, %
1	-0.1924	11.030	-0.1927	11.009	0.15	0.19
2	-1.0425	15.640	-1.0405	15.625	0.19	0.10
3	-3.4175	20.737	-3.4106	20.717	0.20	0.09
4	-1.6897	21.942	-1.6815	21.918	0.48	0.11
5	-10.086	33.729	-10.025	33.652	0.61	0.22
6	-11.680	35.268	-11.571	35.140	0.94	0.36
7	-29.472	65.501	-29.055	65.213	1.43	0.44
8	-34.059	68.942	-34.098	68.745	0.11	0.28
<i>Size of eigenvalue problem</i>						
CMSFR			DREIGN			
60 × 60 complex			516 × 516 real			

Table 4.9: Comparison of eigenvalues for the damped rig model

<i>Z displacements in the 1st eigenvector</i>				
	CMSFR		DREIGN	
#	Real	Imag	Real	Imag
1	0.648E-05	0.574E-07	0.653E-05	0.141E-07
2	0.965E-01	0.177E-03	0.968E-01	0.143E-03
3	0.255E+00	0.333E-03	0.256E+00	0.209E-03
4	0.425E+00	0.657E-03	0.426E+00	0.104E-02
5	0.657E-05	0.485E-07	0.652E-05	0.182E-07
6	0.956E-01	0.126E-03	0.954E-01	0.476E-04
7	0.252E+00	0.205E-03	0.251E+00	0.434E-03
8	0.420E+00	0.401E-03	0.419E+00	0.216E-03
9	0.102E+00	0.132E-03	0.102E+00	0.976E-04
10	0.304E+00	-0.156E-02	0.304E+00	-0.151E-02
11	0.305E+00	-0.165E-02	0.304E+00	-0.163E-02
12	0.104E+00	0.531E-04	0.103E+00	0.694E-04

Table 4.10: Comparison of the 1st eigenvectors for the damped rig model

Chapter 5

Experimental results

The experimental section of this work contains results obtained for the vibration rig (Fig.5.1), which was designed and constructed for the purpose of modelling the vibrations of an engine mounted on a flexible support. Its geometric parameters (in inches) are given in the Appendix B. The material used for all elements, except springs isolators, was steel. The rig contains the four spring isolators a, b, c, d (Fig.5.2) that can be adjusted to provide different damping and stiffness characteristics.

For the experimental determination of stiffness and damping characteristics of the spring isolators the following procedure (Fig.5.3) was used. A vertical impact is applied at the mass m_s and the natural (damped) frequency and logarithmic decrement of the free vertical oscillations of mass m_s is measured.

The natural frequency is obtained by using "Nicolet 660 A" spectrum analyzer and an accelerometer attached to the mass. The Fourier transform feature built into the analyzer is used to determine the natural damped frequency p_s . It is assumed that damping is small (damped and undamped frequencies are close), thus stiffness of the spring can be determined as

$$k_s = p_s^2 m_s$$

The damping coefficient of the equivalent dashpot (Fig. 5.3) is determined as

$$c_s = \frac{1}{\pi} m_s p_s \ln \frac{A_i}{A_{i+1}}$$

where A_i, A_{i+1} are the two consecutive amplitudes of oscillation separated by the period

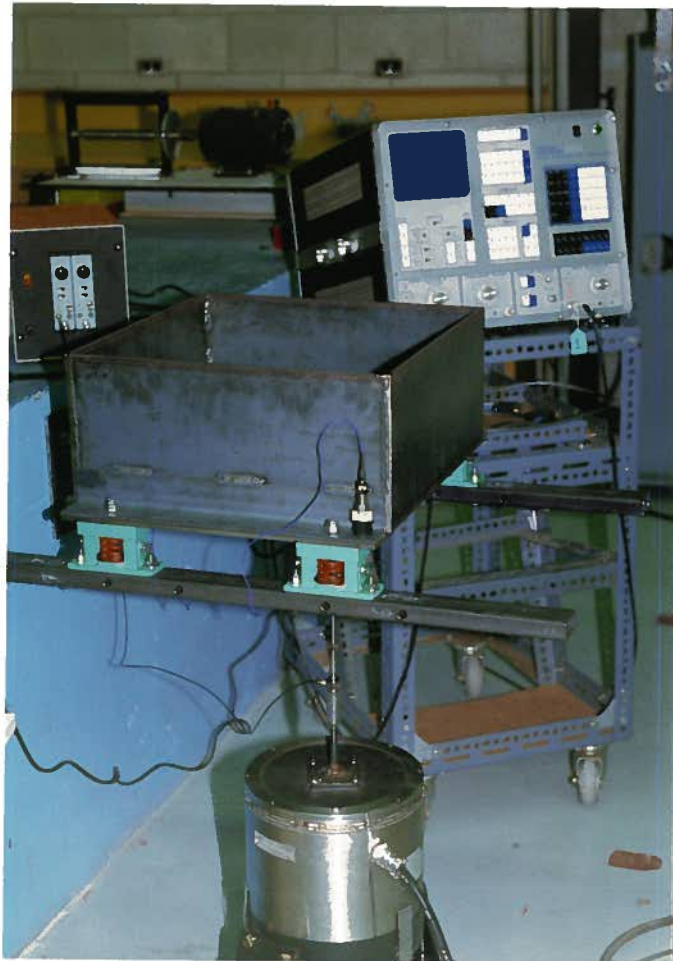


Figure 5.1: Photo of the experimental rig

$$= 2\pi/p_s.$$

These experimentally determined characteristics of the spring isolators (Tables 5.1,5.2) were assigned to the elements a, b, c, d in the finite element model. The first set of damping properties were taken as zero, i.e. the 1st rig model was considered as an undamped system. The free oscillations of the undamped rig were considered at first. The natural frequencies (Table 5.3) were obtained using the "Nicolet" analyzer and piezoelectric accelerometers attached to various points of the rig. It may be seen from Table 4.7 that a good agreement with the analytical results was obtained.

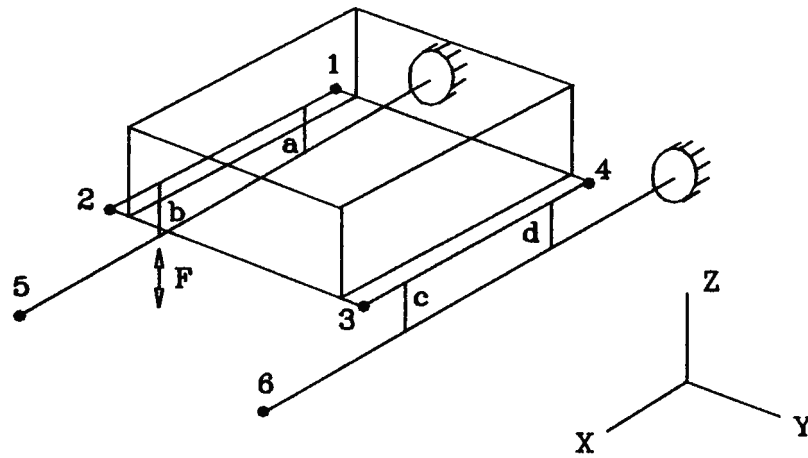


Figure 5.2: Reference points on the test rig

<i>Properties of the 4 isolators</i>		
#	Stiffness, N/mm	Damping coeff-t, N × s/mm
1	12.2	0.
2	14.1	0.
3	12.5	0.
4	11.3	0.

Table 5.1: Stiffness and damping properties of the spring isolators (undamped rig)

<i>Properties of the 4 isolators</i>		
#	Stiffness, N/mm	Damping coeff-t, N × s/mm
1	257.9	0.116
2	314.4	0.180
3	281.9	0.142
4	247.3	0.102

Table 5.2: Stiffness and damping properties of the spring isolators (damped rig)

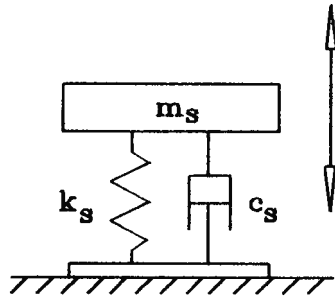


Figure 5.3: Spring isolator characteristic determination

<i>Natural frequencies, Hz</i>		
#	undamped rig	damped rig (with different stiffness)
1	4.65	11.1
2	5.75	15.75
3	6.1	22.5
4	8.20	23.25
5	8.35	35.75
6	9.50	36.75
7	30.25	-
8	30.75	-

Table 5.3: Experimental frequencies for two rig tests

In the second test damping was introduced into the spring isolators (due to the specific construction of the spring isolator the introduction of damping leads to increasing stiffness) and the natural frequencies were measured (Table 5.3). Note the good agreement with the analytical results in Table 4.9. It may be seen that the higher frequencies are associated with quite large real parts. The experimental determination of the higher frequencies (#7,#8) was complicated due to the fast amplitude decay of the free vibration response.

Forced responses due to a sinusoidal vertical force applied to point "b" (Fig.5.2) were

<i>Excitation frequencies, Hz</i>								
	$\omega = 5.9$				$\omega = 6.2$			
	Amplitude		Phase, °		Amplitude		Phase, °	
#	Ex.	An.	Ex.	An.	Ex.	An.	Ex.	An.
1	0.365	0.397	0.	0.	0.565	0.525	180.	180.
2	0.173	0.256	0.	0.	0.494	0.470	180.	180.
3	0.515	0.505	0.	0.	0.403	0.448	180.	180.
4	0.699	0.648	0.	0.	0.483	0.505	180.	180.
5	0.192	0.232	0.	0.	0.112	0.109	180.	180.
6	0.208	0.212	0.	0.	0.161	0.185	180.	180.

Table 5.4: Amplitudes, Phase angles for undamped rig

analyzed for the damped rig. At first an excitation frequency sweep with a constant force amplitude (10 N) was conducted with a rate $\dot{\omega} = 0.2 \text{ Hz/s}$. The measured amplitude of vibration at the point 2 is shown in Fig.5.4. It may be seen that the peaks of the response correspond to the frequencies associated with the eigenvalues (Table 5.3).

Next a sinusoidal vertical excitation at a fixed frequency and force magnitude was applied to the point "b". Comparison of the analytical and experimental steady-state responses (amplitude vector and phase angle vector) for six points of the rig (Fig. 5.2) was conducted. The amplitudes (in dimensionless form) and phase angles are presented in Tables 5.4,5.5 for the undamped rig model and in Tables 5.6,5.7 for the damped one. The experimental phase angles were determined with an accuracy of 5° . It may be seen a good agreement of the experimental and analytical results.

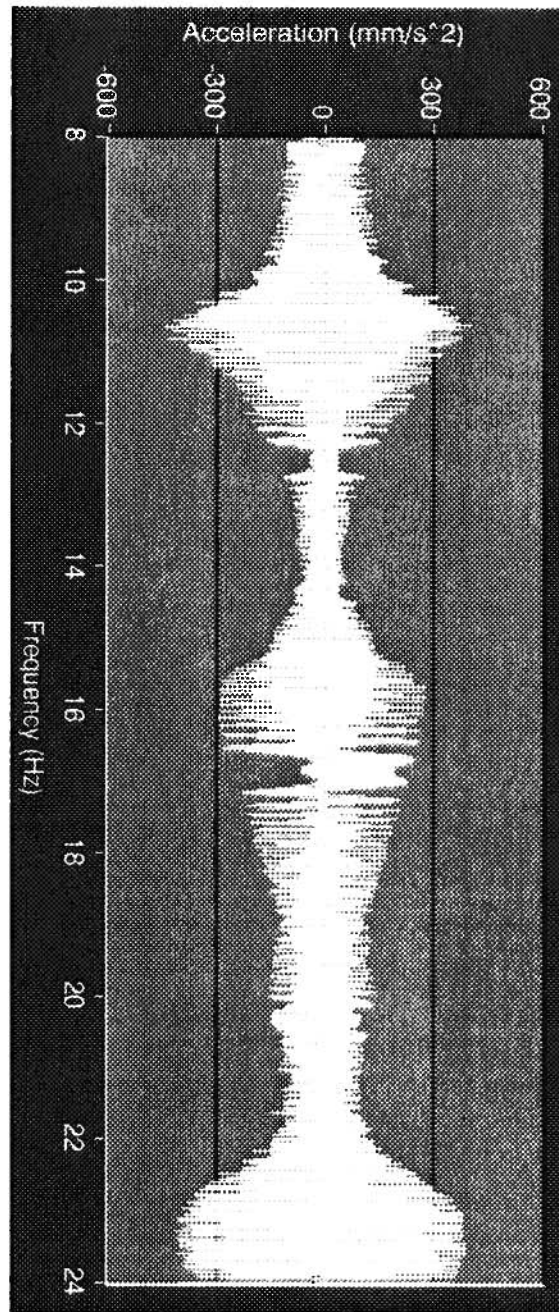


Figure 5.4: 8 - 24 Hz excitation sweep

<i>Excitation frequencies, Hz</i>								
	$\omega = 16.0$				$\omega = 33.0$			
	Amplitude		Phase,°		Amplitude		Phase,°	
#	Ex.	An.	Ex.	An.	Ex.	An.	Ex.	An.
1	0.077	0.089	180.	180.	0.026	0.022	0.	0.
2	0.105	0.118	180.	180.	0.031	0.027	0.	0.
3	0.014	0.022	0.	0.	0.002	0.004	180.	180.
4	0.049	0.056	0.	0.	0.024	0.014	180.	180.
5	0.989	0.986	0.	0.	0.998	0.999	180.	180.
6	0.015	0.020	0.	0.	0.014	0.019	0.	0.

Table 5.5: Amplitudes, Phase angles for undamped rig ... continued

<i>Excitation frequencies, Hz</i>								
	$\omega = 11.0$				$\omega = 16.0$			
	Amplitude		Phase,°		Amplitude		Phase,°	
#	Ex.	An.	Ex.	An.	Ex.	An.	Ex.	An.
1	0.071	0.081	240.	252.	0.248	0.303	242.	249.
2	0.413	0.441	233.	250.	0.441	0.356	247.	245.
3	0.474	0.441	236.	250.	0.300	0.329	77.	74.5
4	0.063	0.083	240.	250.	0.382	0.316	72.	69.6
5	0.530	0.545	248.	251.	0.534	0.541	242.	248.
6	0.559	0.545	233.	250.	0.470	0.527	67.	73.5

Table 5.6: Amplitudes, Phase angles for damped rig

<i>Excitation frequencies, Hz</i>				
$\omega = 24.0$				
#	Amplitude		Phase, °	
	Ex.	An.	Ex.	An.
1	0.373	0.303	253.	249.
2	0.306	0.332	237.	250.
3	0.324	0.328	67.	74.6
4	0.192	0.269	40.	74.7
5	0.621	0.560	243.	253.
6	0.487	0.550	64.	74.7

Table 5.7: Amplitudes, Phase angles for damped rig ... continued

Chapter 6

Summary

Results have been presented that allow the prediction of the effect of damping on the free vibration response of classically damped discrete nongyroscopic systems. The results presented are general in the sense that they consider all possible damping conditions that lead to classically damped systems, which have distinct undamped natural frequencies. For this class of systems it is possible to specify the damping matrix that will result in each mode having prescribed decay factor or damped natural frequency and for that just the knowledge of undamped natural frequencies is required. The equations required to accomplish this task have been presented.

For nonclassically damped systems the free response behaviour is more complex and no general rules concerning the influence of damping on free response characteristics are evident. Characteristics not observed in classically damped systems are shown and discussed. It has been demonstrated that increasing damping can lead to an increase in free response frequency. Modification of damping properties of a system may lead to obtaining of desirable system eigenquantities, free and forced vibration responses.

A component mode synthesis method that enables the determination of eigenquantities (for a given range of interest) has been developed. The use of this method is especially advantageous in the case of large systems, subjected to numerous modifications. The numerical results presented confirm the validity of the method.

It has been shown that the effect of damping properties of the spring isolators of the vibration rig model on transmissibility of motion from the box to the supported beams is

quite significant. Increase of damping constants in the isolators (at the constant stiffness characteristics) leads to a decrease of amplitudes of vibration of the supported beams, in other words, it provides a decrease of transmissibility of motion from the box to the supported beams.

Comparison of analytical and experimental results is presented, which shows good agreement for eigenvalues, and steady-state responses of the vibration rig.

As the future work, the assignment of the optimum range of retained component eigenvectors can be further investigated. Also the displacement compatibility between components can be generalized, i.e., for some types of interfaces the slippage between components can be introduced, which means the assumption of equality of normal relative displacements and discontinuity of relative tangential displacements at the interface.

Bibliography

- [1] Hurty, W. C., "Dynamic Analysis of Structural Systems Using Component Modes," *AIAA Journal*, Vol. 3, April 1965, pp. 678-685.
- [2] Hurty, W. C., "Introduction to Modal Synthesis Techniques," *Synthesis of Vibrating Systems*, ASME booklet, Nov. 1971, pp. 1-13.
- [3] Craig, R. R., and Bampton, M. C. C., "Coupling of Substructures for Dynamic Analysis," *AIAA Journal*, Vol. 6, July 1968, pp. 1313-1319.
- [4] Craig, R. R., and Chang, C., "Free-Interface Methods of Substructure Coupling for Dynamic Analysis," *AIAA Journal*, Vol. 14, No. 8, November 1976, pp. 1633-1635.
- [5] Hintz, R. M., "Analytical Methods in Component Modal Synthesis," *AIAA Journal*, Vol. 13, Aug. 1975, pp. 1007-1016.
- [6] Dowell, E.H., "Free Vibrations of an Arbitrary Structure in Terms of Component Modes," *Journal of Applied Mechanics*, Vol. 39, September 1972, pp. 727-732.
- [7] Goldman, R.L., "Vibration Analysis by Dynamic Partitioning," *AIAA Journal*, Vol. 7, No. 6, June, 1969, pp. 1152-1154.
- [8] Gladwell, G.M.L., "Branch Mode Analysis of Vibrating Systems", *Journal of Sound and Vibration*, Vol. 1, 1964, pp. 41-59.
- [9] Hou, S., "Review of Modal Synthesis Techniques and a New Approach," *Shock and Vibration Bulletin*, Vol. 40, Part 4, Dec. 1969, pp. 25-39.
- [10] MacNeal, R. H., "A Hybrid Method of Component Mode Synthesis," *Computers and Structures*, Vol. 1, Dec. 1971, pp. 581-601.
- [11] Meirovitch, L., "Computational Methods in Structural Dynamics", Sijhoff and Noordhoff International Publishers, Alpen aan den Rijn, The Netherlands, 1980.
- [12] Craig, R. R., "A Review of Time-Domain and Frequency-Domain Component-Mode Synthesis Methods," *International Journal of Analytical and Experimental Modal Analysis*, Vol. 2, No. 2, April 1987, pp. 59-72.
- [13] Smith M. J., "An evaluation of component mode synthesis for modal analysis of finite element models," Ph.D thesis, UBC, Vancouver, B.C., 1993.

- [14] Meirovitch, L., and Hale A.L., "On the Substructure Synthesis Method," *AIAA Journal*, Vol. 19, No. 7, July 1981, pp. 940-947.
- [15] Hale, A.L., and Meirovitch, L., "A General Substructure Synthesis Method for the Dynamic Simulation of Complex Structures," *Journal of Sound and Vibration*, Vol. 69, No. 2, 1980, pp. 309-326.
- [16] Weaver, W., Young, D. H., Timoshenko, S. P., "Vibration Problems in Engineering," John Wiley and Sons, 1990.
- [17] Meirovitch, L., "Elements of Vibration Analysis," McGraw Hill, 1975.
- [18] Thomson, W. T., "Theory of Vibrations with Applications," Prentice Hall Inc., 1981.
- [19] Clough, R. W., Penzien, J., "Dynamics of Structures," McGraw Hill, 1975.
- [20] Craig, R. R., "Structural Dynamics", Macmillan, 1979.
- [21] Bellman R., "Introduction to Matrix Analysis," McGraw-Hill Book Company, Inc., New York, N.Y., 1960.
- [22] Caughey T. K., M. E. J. O'Kelly, "Classical Normal Modes in Damped Linear Dynamic Systems," *Journal of Applied Mechanics*, Vol. 12, 1965, pp. 583-588.
- [23] Bishop R. E. D., Gladwell G. M. L., "An investigation into the theory of resonance testing," *Philosophical Transactions of the Royal Society of London*, Vol. 255, Series A. 1963, pp. 241-280.
- [24] Hasselman, T. K. and Kaplan, A., "Dynamic Analysis of Large Systems by Complex Mode Synthesis," *Journal of Dynamic Systems, Measurement, and Control*, Vol. 96, Series G, 1974, pp. 327-333.
- [25] Beiveau, J., and Soucy, Y., "Damping Synthesis Using Complex Substructure Modes and a Hermitian System Representation," *Proceedings of the AIAA/ASME/ASHE/AHS*, New York, 1985, pp. 581-586.
- [26] Howsman, T., and Craig, R.R., "A Substructure Coupling Procedure Applicable to General Linear Time-Invariant Dynamic Systems," *Proceedings of the AIAA/ASME/ASHE/AHS*, New York, 1984, pp. 164-171.
- [27] Craig, R. R., and Ni, Z., "Component Mode Synthesis for Model Order Reduction of Nonclassically Damped Systems," *J.Guidance*, Vol. 12, July-August. 1989, pp. 577-584.

- [28] Francis, J.G.F., "The QR Transformations, Parts I and II", *The Computer Journal*, Vol. 4, 1961, pp. 265-271, 332-345.
- [29] Kublanovskaya, V.N., "On Some Algorithm for the Solution of the Complete Eigenvalue Problem", *USSR Comput. Math. Math. Phys.*, Vol. 3, 1961, pp. 637-657.
- [30] Rubin, S., "Improved Component-Mode Representation for Structural Dynamic Analysis," *AIAA Journal*, Vol. 13, No. 8, August 1975, pp. 995-1006.
- [31] Martec Limited., "Vibration and Strength Analysis Program (VAST): User's manual," Halifax, N.S.,1990.
- [32] Nicol T., (editor), "UBC Matrix book (A Guide to Solving Matrix Problems)," Computing Centre, UBC, Vancouver, B.C., 1982.

Appendix A

User's Manual for the CMSFR method

The main program in which the CMSFR method was implemented is named VASFIN. It was written by the author of this thesis. The computer language used was FORTRAN-77.

Instructions to run VASFIN (gives the final results)

The following files (* means prefix) are required to prepare to run VASFIN:

1. *.con
2. *.ibn
3. *.rmk
4. *.dam
5. *.mod
6. *.lst
7. *.lms
8. *.ldp

-
1. *.con is ouput file of VASPRE
 2. *.ibn is ouput file of VASPRE
 3. *.rmk is ouput file of VASPRE
 4. *.dam is ouput file of VASDAM
 5. *.mod consists from one line, which contains the system eigenvalue range of interest

and adjustment coefficient r for the selection of component nodes (it is created manually)

6. *.lst contains constraint and weak springs for specified nodes of each component (it is created manually)

7. *.lms contains lumped masses for specified nodes of each component (it is created manually)

8. *.ldp contains lumped dashpots for specified nodes of each component (it is created manually)

The output files after execution of VASFIN are:

1. *.res contains eigenvalues, eigenvectors, the response function of the system.

Instructions to run VASPRES

The following files are required to prepare to run VASPRES:

1. *.gom (= *.gml, copy of *.gml)

2. *.sed

3. *.use

1. *.gom is created from (basic) *.gom files of each component by running VASGEN program

2. *.sed is created from (basic) *.gom files of each component by running VASSED program

3. *.use. The same for all cases, only the first line (title of the problem) can be different.

The output files after execution of VASPRES are:

1. *.con (contains the quantity of components)
2. *.ibn (component connection information)
3. *.rmk (mass, stiffness matrices of components)

Remark.

For VASP, program VAST60 was taken as an initial program [31], which was written in FORTRAN-77. Only subroutine "elems2" was slightly modified and instead of "cms2", subroutine "compox" is used. These modifications were made by the author of this thesis.

Instructions to run VASDAM

The following files are required to prepare to run VASDAM:

1. *.gom (= *.gm2, copy of *.gm2)
2. *.sed
3. *.use

1. *.gom is created from *.gom files of each component by running VASGEN program. Note that *.gom file will be as *.gm2, where damping properties of each component element are governed by two parameters: "modulus of elasticity" and "density". They reflect two factors: i) the damping matrix of the element is proportional to the element stiffness matrix, ii) the damping matrix of the element is proportional to the element mass matrix. The value, e.g., 10^{-7} can be used for these two parameters in order to prescribe zero damping to the elements of each component

2. *.sed (the same as for VASP)
3. *.use (the same as for VASP)

The output files after execution of VASDAM are:

1. *.dam (damping matrices of components)

Remark.

For VASDAM, program VAST60 was taken as an initial program. Only subroutines "assem.2", "elems2" were slightly modified. These modifications were made by the author of this thesis.

Appendix B

Parameters of the vibration rig

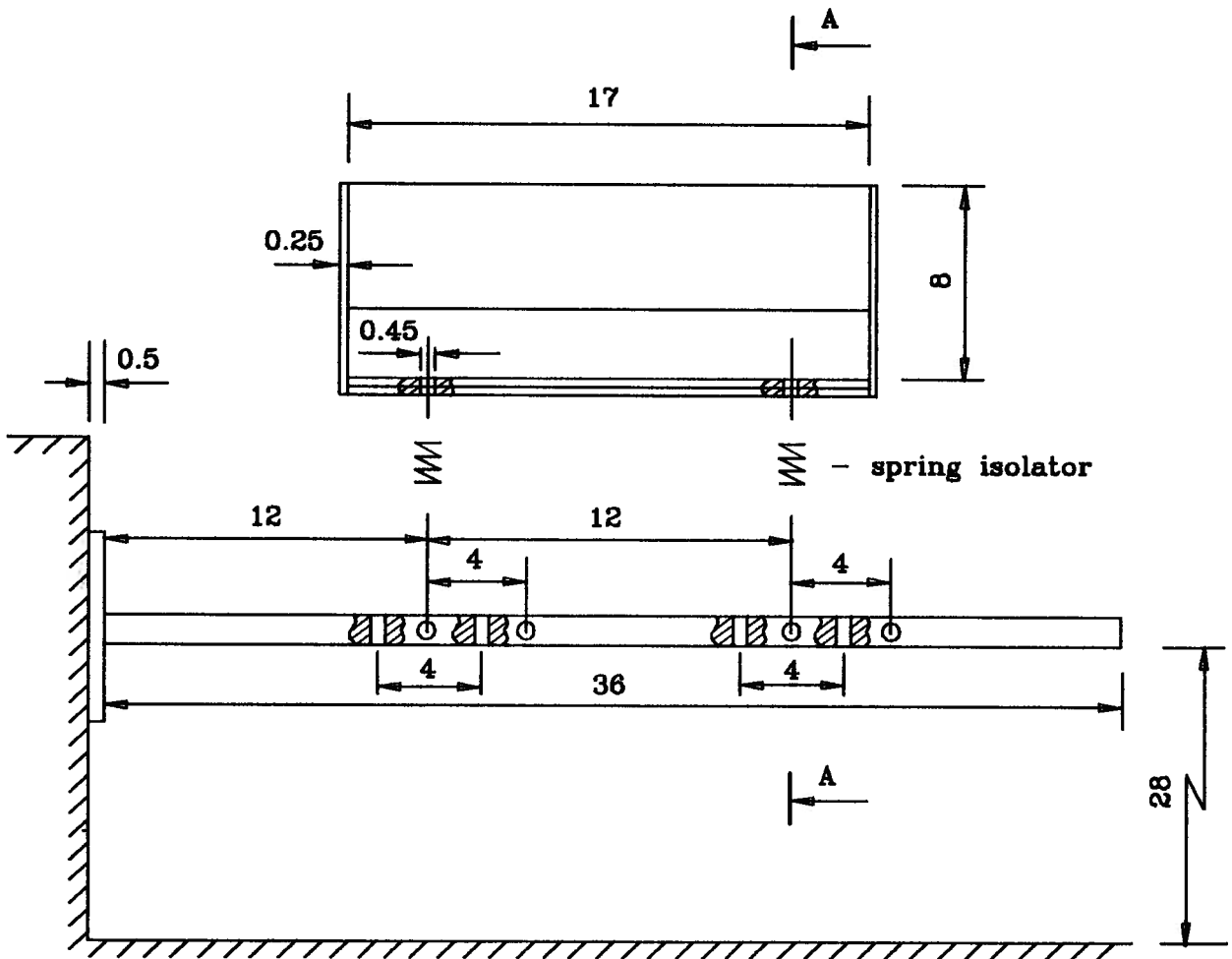


Figure B.1: Vibration rig, side view

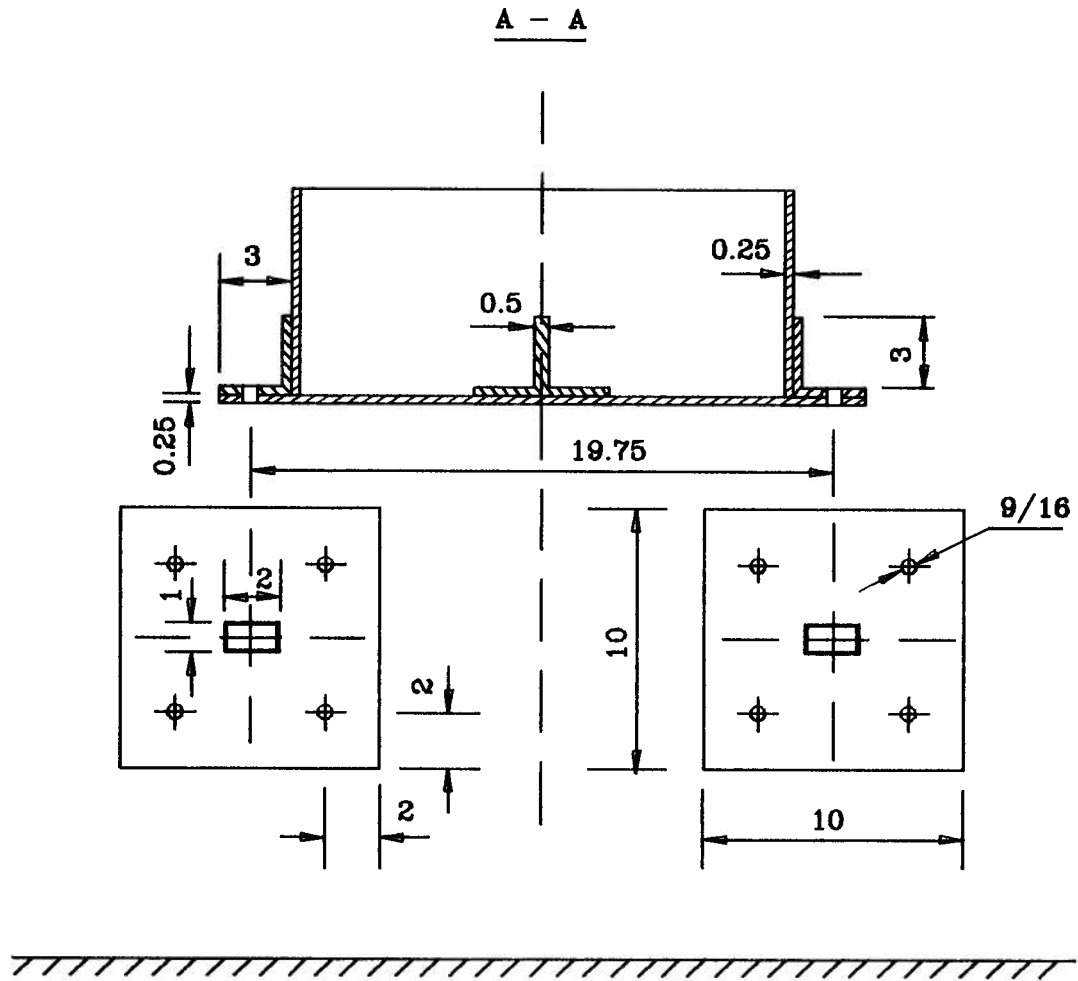


Figure B.2: Vibration rig, front view

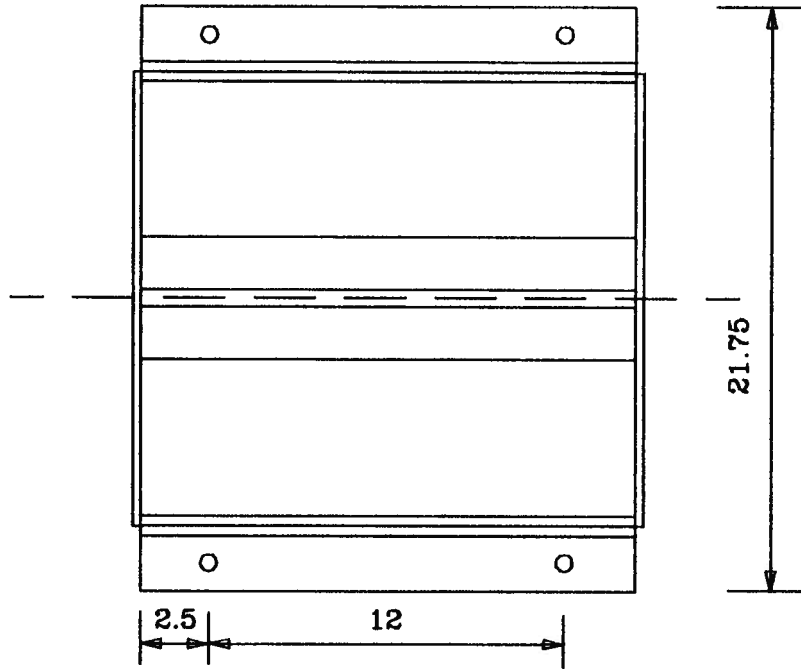


Figure B.3: Vibration rig, top view of the box